



**GEOVANE JUNQUEIRA ALVES**

**DAILY RAINFALL EROSIVITY AS AN INDICATOR OF  
NATURAL DISASTERS APPLIED TO THE MOUNTAINOUS  
REGION OF RIO DE JANEIRO, BRAZIL: CURRENT  
SCENARIO AND FUTURE PROJECTIONS**

**LAVRAS – MG  
2023**

**GEOVANE JUNQUEIRA ALVES**

**DAILY RAINFALL EROSIVITY AS AN INDICATOR OF NATURAL DISASTERS  
APPLIED TO THE MOUNTAINOUS REGION OF RIO DE JANEIRO, BRAZIL:  
CURRENT SCENARIO AND FUTURE PROJECTIONS**

Tese apresentada à Universidade Federal de Lavras, como parte das exigências do Programa de Pós-Graduação em Recursos Hídricos, área de concentração em Hidrologia, para a obtenção do título de Doutor.

Prof. Dr. Carlos Rogério de Mello  
Orientador

**LAVRAS – MG  
2023**

Ficha catalográfica elaborada pelo Sistema de Geração de Ficha Catalográfica da Biblioteca Universitária da UFLA,  
com dados informados pelo(a) próprio(a) autor(a).

Alves, Geovane Junqueira.

Daily rainfall erosivity as an indicator of natural disasters applied to the mountainous region of Rio de Janeiro, Brazil: current scenario and future projections / Geovane Junqueira Alves. – 2021.

65 p. : il.

Orientador: Carlos Rogério de Mello.

Tese (Doutorado) - Universidade Federal de Lavras, 2021.  
Bibliografia.

1. Daily rainfall erosivity. 2. Natural disasters. 3. Brazilian mountainous regions. I. Mello, Carlos Rogério de. II. Título.

**GEOVANE JUNQUEIRA ALVES**

**DAILY RAINFALL EROSIVITY AS AN INDICATOR OF NATURAL DISASTERS  
APPLIED TO THE MOUNTAINOUS REGION OF RIO DE JANEIRO, BRAZIL:  
CURRENT SCENARIO AND FUTURE PROJECTIONS**

**EROSIVIDADE DA PRECIPITAÇÃO DIÁRIA COMO UM INDICADOR DE  
DESASTRES NATURAIS APLICADO NA REGIÃO SERRANA DO ESTADO DO  
RIO DE JANEIRO, BRASIL: CENÁRIO ATUAL E PROJEÇÕES FUTURAS**

Tese apresentada à Universidade Federal de Lavras, como parte das exigências do Programa de Pós-Graduação em Recursos Hídricos, área de concentração em Hidrologia, para a obtenção do título de Doutor.

APROVADO em 31 de maio de 2021.

Dr. Michael Silveira Thebaldi  
Dr. Livia Alves Alvarenga  
Dr. Junior Cesar Avanzi  
Dr. Sly Wongchuig Correa

Federal University of Lavras (UFLA)  
Federal University of Lavras (UFLA)  
Federal University of Lavras (UFLA)  
University of Grenoble Alpes (UGA)



Prof. Dr. Carlos Rogério de Mello  
Orientador

**LAVRAS – MG  
2023**

## AGRADECIMENTOS

Acima de tudo, à Deus, pela vida, e por sempre me guiar por seus caminhos, dando-me coragem para enfrentar todos os obstáculos que neles se encontram.

Aos meus pais, José Carlito (*in memoriam*) e Elizete que sempre me ensinaram a praticar o bem. À minha irmã, Marília, pela amizade e cumplicidade.

À minha esposa, Mariana, por mostrar-se companheira e por sempre me amparar nas horas difíceis. Sem você essa conquista não seria possível.

Ao meu orientador, e amigo, Dr. Carlos Rogério de Mello, pelo exemplo de profissionalismo, orientação e amizade. Tenho gratidão eterna pelos seus exemplos e ensinamentos.

Aos meus familiares, em especial ao meu tio, José Alves Junqueira Junior, por me aconselhar nas horas difíceis.

À Universidade Federal de Lavras (UFLA), e ao Programa de Pós-Graduação em Recursos Hídricos, pela formação profissional e estrutura física oferecida.

A todos os professores que tive o prazer de conhecer, e que sempre me instigaram pela busca do conhecimento. A cada dia tento ser um pouco de cada um de vocês.

À Coordenação de Aperfeiçoamento de Pessoal do Nível Superior (CAPES) pelo apoio financeiro.

E por fim, a todos aqueles que de alguma maneira colaboraram para a conclusão deste trabalho.

Muito obrigado!

## RESUMO

Desastres naturais são definidos como decorrência de eventos naturais extremos que causam impactos significativos no equilíbrio social, econômico e ambiental. Assim, índices de alerta para prevenir ou minimizar os impactos causados por desastres naturais têm se tornando um dos grandes desafios do século XXI. Nesse contexto, e considerando que alguns índices baseados apenas na precipitação têm-se mostrados ineficientes, a erosividade da chuva, calculada como função da energia dissipada pelo impacto de gotas sobre a superfície, tem grande potencial para aplicação em estudos relacionados a deslizamentos de encostas e inundações. Assim, a erosividade de chuvas diárias ( $R_{\text{dia}}$ ) é um índice promissor de ser aplicado como alerta de ocorrência de desastres naturais permitindo também analisar o comportamento destes eventos frente às mudanças climáticas. Neste aspecto, os objetivos deste estudo foram: i) modelar o  $R_{\text{dia}}$  através de um modelo sazonal para a Região Serrana do Estado do Rio de Janeiro (RSERJ), que tem sido uma das regiões mais afetadas por desastres naturais no Brasil; ii) adequar, com base em eventos catastróficos ocorridos nas últimas duas décadas, limiares do índice  $R_{\text{dia}}$  que classificam os eventos de acordo com os respectivos impactos observados; iii) aplicar o modelo sazonal ajustado para a estimativa de  $R_{\text{dia}}$  considerando dois cenários de emissão de gases de efeito estufa (RCP 4.5 e 8.5) e o modelo climático HadGEM2-ES regionalizado para a escala de 5 km ao longo do século XXI; iv) mapear a erosividade máxima diária ( $R_{\text{maxdia}}$ ) para avaliar a susceptibilidade da região, conforme os limiares estabelecidos, ao longo do século e; v) analisar espacialmente a frequência de ocorrência dos valores de  $R_{\text{dia}}$  causadores de desastres naturais considerando as projeções futuras. O modelo ajustado apresentou resultado satisfatório, permitindo sua aplicação como estimador da sazonalidade do  $R_{\text{dia}}$  na RSERJ. Eventos que resultaram em  $R_{\text{dia}} > 1.500 \text{ MJ.ha}^{-1}.\text{mm.h}^{-1}.\text{dia}^{-1}$  foram aqueles com o maior número de óbitos nesta região. O mapeamento do  $R_{\text{maxdia}}$  demonstrou que toda a RSERJ apresentou nos últimos 30 anos valores classificados como causadores de grandes desastres naturais e ainda é altamente susceptível à ocorrência destes grandes desastres ao longo do século XXI, com intensificação no período de 2040-2071. As áreas urbanas de Nova Friburgo e Petrópolis foram as que apresentaram maior frequência de eventos na faixa  $1.000 < R_{\text{maxdia}} < 1.500 \text{ MJ.ha}^{-1}.\text{mm.h}^{-1}.\text{dia}^{-1}$ . O período de 2011-2040 é o que apresentou a menor frequência de eventos, com concentração de  $R_{\text{maxdia}} < 1.000 \text{ MJ.ha}^{-1}.\text{mm.h}^{-1}.\text{dia}^{-1}$ . Os índices  $R_{\text{dia}}$  se mostraram promissores como indicadores de desastres naturais, sendo mais efetivo do que os usualmente utilizados, os quais são baseados somente em quantidade (mm) e intensidade ( $\text{mm.h}^{-1}$ ) da chuva.

**Palavras-chave:** Erosividade diária. Desastres naturais. Regiões serranas brasileiras. Índices de alertas de precipitação. Mudanças climáticas.

## ABSTRACT

Natural disasters result from extreme natural events that cause significant impacts on the social, economic, and environmental balance. Thus, alert indices to prevent or minimize the impacts caused by natural disasters have become one of the most significant challenges of the twenty-first century. In this context and considering that some indices based only on precipitation have been shown to be inefficient, the rainfall erosivity, calculated as a function of the energy dissipated by the impact of drops on the surface, has great potential for application in studies related to landslides and floods. Thus, daily rainfall erosivity ( $R_{\text{day}}$ ) are promising indices to be applied as alerts of the occurrence of natural disasters, also allowing us to analyze the behavior of these events in the face of climate change. Therefore, this study aimed to i) model the  $R_{\text{day}}$  through a seasonal model for the mountainous region of the state of Rio de Janeiro (RSERJ), one of the regions most affected by natural disasters in Brazil; ii) adapt thresholds of the  $R_{\text{day}}$  indices that classify the events according to their observed impacts based on catastrophic events that have occurred in the last two decades; iii) apply the adjusted seasonal model to calculate  $R_{\text{day}}$  considering two greenhouse gas emission scenarios (RCP 4.5 and 8.5) and the regionalized HadGEM2-ES climate model for the 5 km scale throughout the twenty-first century; iv) map the maximum daily rainfall erosivity ( $R_{\text{maxdia}}$ ) to evaluate the susceptibility of the region, according to the established thresholds throughout the century; and v) spatially analyze the frequency of occurrence of  $R_{\text{day}}$  values causes of natural disasters considering future projections. The adjusted model showed a satisfactory result, allowing its application as an estimator of the seasonality of the  $R_{\text{day}}$  at RSERJ. Events that resulted in  $R_{\text{day}} > 1,500 \text{ MJ}\cdot\text{ha}^{-1}\cdot\text{mm}\cdot\text{h}^{-1}\cdot\text{day}^{-1}$  presented this region's highest number of deaths. The mapping of  $R_{\text{maxdia}}$  showed that the entire RSERJ presented values classified as causing major natural disasters in the last 30 years and is still highly susceptible to the occurrence of major natural disasters throughout the twenty-first century, with intensification from 2040 to 2071. The urban areas of Nova Friburgo and Petrópolis showed the highest frequency of events in the range  $1,000 < R_{\text{maxdia}} < 1,500 \text{ MJ}\cdot\text{ha}^{-1}\cdot\text{mm}\cdot\text{h}^{-1}\cdot\text{day}^{-1}$ . The period between 2011 and 2040 presented the lowest frequency of events, with a concentration of  $R_{\text{maxdia}} < 1,000 \text{ MJ}\cdot\text{ha}^{-1}\cdot\text{mm}\cdot\text{h}^{-1}\cdot\text{day}^{-1}$ . The  $R_{\text{day}}$  indices were promising indicators of natural disasters, being more effective than those generally used, based only on rainfall quantity (mm) and intensity ( $\text{mm}\cdot\text{h}^{-1}$ ).

**Keywords:** Daily rainfall erosivity. Natural disasters. Brazilian mountainous regions. Rainfall warning system. Climate change.

## SUMÁRIO

	<b>1<sup>st</sup> CHAPTER – GENERAL INTRODUCTION.....</b>	<b>8</b>
<b>1</b>	<b>GENERAL INTRODUCTION .....</b>	<b>8</b>
	<b>REFERENCES .....</b>	<b>12</b>
	<b>2<sup>nd</sup> CHAPTER - ARTICLES.....</b>	<b>15</b>
	<b>ARTICLE 1 - NATURAL DISASTER IN THE MOUNTAINOUS REGION OF RIO DE JANEIRO STATE, BRAZIL: ASSESSMENT OF THE DAILY RAINFALL EROSIVITY AS AN EARLY WARNING INDEX.....</b>	<b>15</b>
	<b>ARTICLE 2 - RAINFALL DISASTERS UNDER THE CHANGING CLIMATE: A CASE STUDY FOR THE RIO DE JANEIRO MOUNTAINOUS REGION.....</b>	<b>48</b>



## 1<sup>ST</sup> CHAPTER – GENERAL INTRODUCTION

### 1 GENERAL INTRODUCTION

Natural disasters are defined as the result of extreme natural events which cause negative impacts on the society, economy, and environment (ALEXANDER, 2018). Among the natural disasters that most affect the people, floods and landslides caused by intense rainfall are responsible for thousands of deaths worldwide.

The increase in the frequency and intensity of extreme rainfall in Brazil, combined with the high degree of susceptibility of the population in risk areas has triggered disasters, such as landslides and floods (FERNANDES and RODRIGUES, 2018; AMORIM and CHAFFE, 2019; MELLO et al., 2020). Within this context, one of the regions more affected by landslides and floods is the mountainous region of the state of Rio de Janeiro (MRRJ), which is one of the most vulnerable areas to the natural disasters in Brazil (BRASIL, 2012; FREITAS et al., 2012; BITAR, 2014; OLIVEIRA et al., 2016). In addition, in this region the influence of the South Atlantic Convergence Zone (SACZ) and the orographic influence coexist, resulting in frequent extreme rainfall events (BRITO et al., 2016; ANDRÉ et al., 2008). Thus, it can be said that, besides the higher frequency of extreme events, they can potentially affect regions more vulnerable to these natural disasters, leading to more significant consequences.

Landslides were triggered by extreme rainfall events between January 11 and 12, 2011, causing the so-called “mega disaster” in the MRRJ, where seven municipalities declared situation of public emergency (VASSOLER, 2013; CARDOZO and MONTEIRO, 2019). This event is considered the worst natural disaster in Brazil’s history (CASTILHO et al., 2012; CARDOZO and MONTEIRO, 2019), not only because of the number of deaths, but also the significant damages in the economy and infrastructure. In Nova Friburgo, for example, the total number of fatalities related to landslides was 434 (205 women and 228 men) (CARDOZO et al., 2018; CARDOZO and MONTEIRO, 2019; OLIVEIRA et al., 2016). This represents more than 47% of the fatalities in the “mega disaster”.

Although the “mega disaster” generated the most destructive landslides ever observed in Brazil, events with similar characteristics have already occurred at Rio de Janeiro state in the years of 1966, 1967, 1988 and 1996 (MEIS and SILVA, 1968; BARATA, 1969; JONES, 1973; LACERDA, 1997, 2007).

In view of the above-mentioned, some authors have assessed the efficiency of Early Warning System (EWS) indicators in reducing risks in the region, mainly related to economic impacts and fatalities (WEBSTER, 2013; ALVALÁ et al., 2019). Guzzetti et al. (2007) studied indicators that identify vulnerability to natural disasters, claiming that a good indicator should be based on the total precipitation amount, the rainfall intensity, the antecedent soil moisture, and the characteristics of the slopes.

However, despite the difficulty in obtaining all the above-mentioned variables (geological, geomorphological, climatic and hydrological) and gathering them in a single value as an alert index that can be used as an EWS, indexes have been applied to relate extreme precipitation events (accumulated and intensity) with the human and material damages caused (XU et al., 2014; CALVELLO et al., 2015; OLIVEIRA et al., 2016) since it is known that precipitation is the factor that triggers the most of natural disasters (GUZZETTI et al., 2007). In addition, the forecasting of precipitation can be made 48 or even 72 hours before the occurrence of the event (OLIVEIRA et al., 2016), which is enough time for the authorities to assess the characteristics of the event and warn the population of imminent risks.

Some indexes have been widely used in Brazil and in the world, such as the accumulated precipitation in the last 24, 48, 72 and 96 hours (SILVA et al., 2020), the precipitation intensity (mm/h), or even such variables evaluated simultaneously. However, some of these indicators have shown to be inefficient.

In this context, rainfall erosivity when applied in a daily scale, seems to be a good index for natural disasters as it encompasses the impacts caused by the impact of raindrops and the energy dissipated by them on the soil surface (MELLO et al. 2020). It was proposed and defined by Wischmeier and Smith (1958) as the product between the kinetic energy of raindrops and the maximum rainfall intensity in 30 consecutive minutes ( $I_{30}$ ), designated as  $EI_{30}$ .

The original method for calculating  $EI_{30}$  for a given rainfall event ( $E_c \times I_{30}$ ) requires rainfall records with a temporal resolution  $\leq 15$ -min (WISCHMEIER and SMITH, 1978). However, such records are difficult to access and obtain, usually due to an insufficient number of stations (MELLO et al., 2020; XIE et al., 2016).

To apply a model for estimating daily rainfall erosivity based on daily rainfall data (since is much more accessible and spatially distributed) is essential to better understand the role of extreme precipitation events on natural disasters (MELLO et al., 2020). Therefore, Yu and Rosewell (1996) proposed a mathematical approach to estimate daily rainfall erosivity.

This approach is capable of estimating the daily erosivity considering the seasonality of the rainfall erosivity throughout the year. Furthermore, this approach using daily rainfall data makes it possible to evaluate the behavior of daily erosivity influenced by climate change, since the regionalized data by Eta model is capable of estimate rainfall in daily time resolution.

Climate change and its impacts on the magnitude and frequency of natural disasters are still uncertain, especially in regions with significant orographic influences (CHOU et al. 2014). In the last decades, it has been observed that natural disasters mostly landslides and floods have become more frequent and severe (CEPED, 2013), mainly in mountainous regions of Brazil (MELLO et al. 2020). These impacts are due to the evident increase in the intensity and frequency of extreme rainfall events (IPCC, 2013), together with the rapid population, economic and disordered urban growth.

The most important factor influenced by climate change which will affect a region's vulnerability to the natural disasters, are changes in the rainfall pattern. In tropical and subtropical regions, for example, a possible increase in the amount of precipitation is expected for specific periods of the year throughout the 21st century (MELLO et al. 2015).

Some studies have assessed the influence of climate change in erosivity on monthly and annual scales (NEARING 2001; ZHANG et al., 2010; SEGURA et al., 2014; MELLO et al., 2015; RIQUETTI et al., 2020), but none has evaluated these changes based on daily scale ( $R_{\text{day}}$ ).

Therefore, two articles were developed to compose the present thesis that has as general objective to study the daily rainfall erosivity as a tool for natural disasters in mountain regions.

The first article is entitled "*Natural disaster in the mountainous region of Rio de Janeiro state, Brazil: Assessment of the daily rainfall erosivity as an early warning index*", and its purpose is to model the daily rainfall erosivity index ( $R_{\text{day}}$ ) using a seasonal model for the MRRJ. Based on this index, the other objective was to improve an indicator, which could be applied as an Early Warning System (EWS) for natural disasters in this region. This index is capable of to identify areas that are vulnerable to natural disasters, being more sensitive than others that are associate with only the total precipitation and the mean rainfall intensity. Finally, it was compared to other indexes that have been used by government warning systems aiming to demonstrate that  $R_{\text{day}}$  has great potential to be applied instead.

The second article, entitled "*Rainfall disasters under the changing climate: a case study for the Rio de Janeiro mountainous region*", objectives: i) to apply a  $R_{\text{day}}$  seasonal

model for the Mountain Region of Rio de Janeiro (MRRJ) throughout the 21st century, applying data simulated by the MCG HadGEM2-ES, regionalized by the ETA-CPTEC model on the spatial scale of 5 km, considering the RCP4.5 and 8.5 IPCC (2013) scenarios; ii) map the maximum daily rainfall erosivity ( $R_{\text{maxday}}$ ) to assess, based on the  $R_{\text{day}}$  indice, the most vulnerable regions throughout the present century and; iii) spatially the frequency of occurrence of  $R_{\text{maxday}}$  values throughout the 21st century.

Thus, it is essential to note that this study highlights two pioneer aspects: i) the study of climate change and its influence on the values of  $R_{\text{day}}$ ; and ii) use of the rainfall erosivity as an index of extreme events and their variations due to climate changes throughout the 21st century.

## REFERENCES

ALEXANDER, David. **Natural disasters**. Routledge, 2018.

ALVALÁ R.C.S. et al. Mapping characteristics of at-risk population to disasters in the context of Brazilian early warning system. **International Journal of Disaster Risk Reduction**, v. 41, p. 101326, 2019.

AMORIM, Pablo Borges; CHAFFE, Pedro B. Towards a comprehensive characterization of evidence in synthesis assessments: the climate change impacts on the Brazilian water resources. **Climatic Change**, v. 155, n. 1, p. 37-57, 2019.

ANDRÉ, Romisio Geraldo Bouhid et al. Identificação de regiões pluviometricamente homogêneas no estado do Rio de Janeiro, utilizando-se valores mensais. **Revista Brasileira de Meteorologia**, v. 23, n. 4, p. 501-509, 2008.

BARATA, F. E. Landslides in the tropic region of Rio de Janeiro. In: **Proc. 7th Internal Conference on Soil Mechanics and Foundation Engng.** 1969. p. 507-516.

BITAR, Omar Yazbek. **Cartas de suscetibilidade a movimentos gravitacionais de massa e inundações-1: 25.000: nota técnica explicativa**. IPT; CPRM, 2014.

BRASIL, Reconhecimento dos Solos do Estado. Seleção dos Municípios Críticos a Deslizamentos–Nota Explicativa. **Companhia de Pesquisa de Recursos Minerais–CPRM. Ministério das Minas e Energia. Rio de Janeiro**, 2012.

BRITO, Thábata T. et al. Multivariate analysis applied to monthly rainfall over Rio de Janeiro state, Brazil. **Meteorology and Atmospheric Physics**, v. 129, n. 5, p. 469-478, 2017.

CALVELLO, Michele et al. The Rio de Janeiro early warning system for rainfall-induced landslides: analysis of performance for the years 2010–2013. **International journal of disaster risk reduction**, v. 12, p. 3-15, 2015.

CARDOZO, Claudia Paola; LOPES, Eymar Silva Sampaio; MONTEIRO, Antônio Miguel Vieira. Shallow landslide susceptibility assessment using SINMAP in Nova Friburgo (Rio de Janeiro, Brazil). **Revista Brasileira de Cartografia**, v. 70, n. 4, p. 1206-1230, 2018.

CARDOZO, Claudia Paola; MONTEIRO, Antônio Miguel Vieira. ASSESSING SOCIAL VULNERABILITY TO NATURAL HAZARDS IN NOVA FRIBURGO, RIO DE JANEIRO MOUNTAIN REGION, BRAZIL. 2019.

CASTILHO, LV de; OLIVEIRA, P.; FABRIANI, Carmen Beatriz. Análise de uma tragédia ambiental e a participação da população no equacionamento dos problemas de moradia: um estudo de caso da tragédia na região serrana do Rio de Janeiro. **VI ENCONTRO NACIONAL DA ANPPAS. Belém-PA**, 2012.

CEPED, 2013. Atlas Brasileiro de Desastres Naturais: 1991-2010, second ed. Ceped, Santa Catarina.

CHOU, Sin Chan et al. Evaluation of the Eta simulations nested in three global climate models. **American Journal of Climate Change**, v. 3, n. 05, p. 438, 2014.

FERNANDES, Laís G.; RODRIGUES, Regina R. Changes in the patterns of extreme rainfall events in southern Brazil. **International Journal of Climatology**, v. 38, n. 3, p. 1337-1352, 2018.

FREITAS, Carlos Machado de et al. Vulnerabilidade socioambiental, redução de riscos de desastres e construção da resiliência: lições do terremoto no Haiti e das chuvas fortes na Região Serrana, Brasil. **Ciência & Saúde Coletiva**, v. 17, p. 1577-1586, 2012.

GUZZETTI, Fausto et al. Rainfall thresholds for the initiation of landslides in central and southern Europe. **Meteorology and atmospheric physics**, v. 98, n. 3, p. 239-267, 2007.

IPCC (2013) Climate change 2013: the physical science basis. Contribution of Working Group I to the Fifth Assessment Report of the Intergovernmental Panel on Climate Change. In: Stocker TF, Qin D, Plattner G-K, Tignor M, Allen SK, Boschung J, Nauels A, Xia Y, Bex V, Midgley PM (eds). Cambridge University Press, Cambridge

JONES, Fred O. **Landslides of Rio de Janeiro and the Serra das Araras escarpment, Brazil**. USGPO, 1973.

LACERDA, Willy A. Stability of natural slopes along the tropical coast of Brazil. In: **Symposium on Recent Developments in Soil and Pavement Mechanics**. CAPES-Fundação Coordenação do Aperfeiçoamento de Pessoal de Nível Superior; CNPq-Conselho Nacional de Desenvolvimento Científico e Tecnológico; FAPERJ-Fundação de Amparo a Pesquisa do Estado do Rio de Janeiro; FINEP-Financiadora de Estudos e Projetos. 1997.

LACERDA, Willy A. Landslide initiation in saprolite and colluvium in southern Brazil: Field and laboratory observations. **Geomorphology**, v. 87, n. 3, p. 104-119, 2007.

MEIS, M. R. M.; SILVA, JX da. Mouvements de masse récents, aRio de Janeiro: Une étude de géomorphologie dynamique. **Revue de Géomorphologie Dynamique**, v. 18, p. 145-152, 1968.

MELLO, Carlos Rogério et al. Assessing the climate change impacts on the rainfall erosivity throughout the twenty-first century in the Grande River Basin (GRB) headwaters, Southeastern Brazil. **Environmental Earth Sciences**, v. 73, n. 12, p. 8683-8698, 2015.

MELLO, Carlos Rogério et al. Daily rainfall erosivity as an indicator for natural disasters: assessment in mountainous regions of southeastern Brazil. **Natural Hazards**, v. 103, p. 947-966, 2020.

NEARING, Mark A. Potential changes in rainfall erosivity in the US with climate change during the 21st century. **Journal of soil and water conservation**, v. 56, n. 3, p. 229-232, 2001.

- OLIVEIRA, Nathalia Silva et al. Correlation between rainfall and landslides in Nova Friburgo, Rio de Janeiro—Brazil: a case study. **Environmental Earth Sciences**, v. 75, n. 20, p. 1-12, 2016.
- RIQUETTI, Nelva B. et al. Rainfall erosivity in South America: Current patterns and future perspectives. **Science of the Total Environment**, v. 724, p. 138315, 2020.
- SEGURA, Catalina et al. Potential impacts of climate change on soil erosion vulnerability across the conterminous United States. **Journal of Soil and Water Conservation**, v. 69, n. 2, p. 171-181, 2014.
- SILVA, Rodrigo Cesar; MENDES, Rodolfo Moreda; FISCH, Gilberto. Future scenarios (2021-2050) of extreme precipitation events that trigger landslides—a case study of the Paraitinga River watershed, SP, Brazil. **Ambiente e Agua-An Interdisciplinary Journal of Applied Science**, v. 15, n. 7, p. 1-18, 2020.
- VASSOLER, R. Ações da vigilância epidemiológica nos desastres naturais. Experiência na Região Serrana em 2011. **Disp. em:** < <http://www.riocomsaude.rj.gov.br/Publico/MostrarArquivo.aspx>, 2013.
- WEBSTER, Peter J. Improve weather forecasts for the developing world. **Nature**, v. 493, n. 7430, p. 17-19, 2013.
- WISCHMEIER, Walter H.; SMITH, Dwight D. Rainfall energy and its relationship to soil loss. **Eos, Transactions American Geophysical Union**, v. 39, n. 2, p. 285-291, 1958.
- WISCHMEIER, Walter H.; SMITH, Dwight David. **Predicting rainfall erosion losses: a guide to conservation planning**. Department of Agriculture, Science and Education Administration, 1978.
- XIE, Yun et al. Models for estimating daily rainfall erosivity in China. **Journal of Hydrology**, v. 535, p. 547-558, 2016.
- XU, Lifen; MENG, Xiangwei; XU, Xuegong. Natural hazard chain research in China: A review. **Natural hazards**, v. 70, n. 2, p. 1631-1659, 2014.
- YU, B.; ROSEWELL, C. J. Rainfall erosivity estimation using daily rainfall amounts for South Australia. **Soil Research**, v. 34, n. 5, p. 721-733, 1996.
- ZHANG, Y.-G. et al. Projected rainfall erosivity changes under climate change from multimodel and multiscenario projections in Northeast China. **Journal of hydrology**, v. 384, n. 1-2, p. 97-106, 2010.

**2<sup>ND</sup> CHAPTER - ARTICLES****ARTICLE 1 - NATURAL DISASTER IN THE MOUNTAINOUS REGION OF RIO DE JANEIRO STATE, BRAZIL: ASSESSMENT OF THE DAILY RAINFALL EROSIVITY AS AN EARLY WARNING INDEX**

Article published in the journal *International Soil and Water Conservation Research*, ISSN: 2095-6339, being published according to the publication rules.



1 **Natural disaster in the mountainous region of Rio de Janeiro state, Brazil: assessment of**  
2 **the daily rainfall erosivity as an early warning index**

3  
4 **Abstract**

5         Rainfall erosivity is defined as the potential of rain to cause erosion. It has great  
6 potential for application in studies related to natural disasters, in addition to water erosion.  
7 The objectives of this study were: i) to model the  $R_{\text{day}}$  using a seasonal model for the  
8 Mountainous Region of the State of Rio de Janeiro (MRRJ); ii) to adjust thresholds of the  $R_{\text{day}}$   
9 index based on catastrophic events which occurred in the last two decades; and iii) to map the  
10 maximum daily rainfall erosivity ( $R_{\text{maxday}}$ ) to assess the region's susceptibility to rainfall  
11 hazards according to the established  $R_{\text{day}}$  limits. The fitted  $R_{\text{day}}$  model presented a satisfactory  
12 result, thereby enabling its application as a  $R_{\text{day}}$  estimate in MRRJ. Events that resulted in  $R_{\text{day}}$   
13  $> 1,500 \text{ MJ}\cdot\text{ha}^{-1}\cdot\text{mm}\cdot\text{h}^{-1}\cdot\text{day}^{-1}$  were those with the highest number of fatalities. The spatial  
14 distribution of  $R_{\text{maxday}}$  showed that the entire MRRJ has presented values that can cause major  
15 rainfall. The  $R_{\text{day}}$  index proved to be a promising indicator of rainfall disasters, which is more  
16 effective than those normally used that are only based on quantity (mm) and/or intensity  
17 ( $\text{mm}\cdot\text{h}^{-1}$ ) of the rain.

18 **Keywords:** Daily rainfall erosivity; rainfall hazards; Brazilian mountainous regions; rainfall  
19 warning system.

20

## 21 1 INTRODUCTION

22           Rainfall erosivity is an index that encompasses the impacts caused by the raindrops  
23 impact and the energy dissipated on the soil surface. It was proposed and defined by  
24 Wischmeier and Smith (1958) as the product between the kinetic energy of raindrops and the  
25 maximum rainfall intensity in 30 consecutive minutes ( $I_{30}$ ), designated as  $EI_{30}$ . Its calculation  
26 requires rainfall data recorded with a temporal resolution  $\leq 15$ -min. However, such records  
27 are difficult to access and obtain, usually due to an insufficient number of stations in  
28 developing countries (Mello et al., 2015).

29           To develop a model for estimating daily rainfall erosivity ( $R_{\text{day}}$ ) based on daily rainfall  
30 data is essential to better understand the role of extreme rainfall on natural disasters (Mello et  
31 al., 2020) since daily rainfall data is much more accessible and spatially distributed than those  
32 with temporal resolutions  $\leq 15$ -minute. Therefore, a model to estimate  $R_{\text{day}}$  was initially  
33 proposed by Richardson et al. (1983), with the inconvenience of having to fit different models  
34 for each month. In addition, these models tend to underestimate the  $R_{\text{day}}$  (Angulo-Martinez  
35 and Beguería, 2009). To overcome these limitations, Yu and Rosewell (1996) proposed a  
36 mathematically more advanced approach by introducing a sinusoidal function to model the  
37 seasonality of rainfall erosivity. This approach can estimate  $R_{\text{day}}$  considering the period of the  
38 year (biweekly or monthly periods). This is a hypothesis that considers that the same  
39 precipitation can generate different  $R_{\text{day}}$  according to the period of year, which is relevant in  
40 regions with a seasonal climate.

41           The increase in the frequency and intensity of extreme rainfall in Brazil, combined  
42 with the high degree of susceptibility of the population in risk areas has triggered rainfall  
43 disasters (Fernandes and Rodrigues, 2018; Amorim and Chaffe, 2019; Mello et al., 2020),  
44 with a high number of fatalities (CEPED, 2013). The geomorphological and pedological  
45 characteristics associated with changes in land use (especially deforestation of the Atlantic

46 Forest) (Freitas et al., 2012) and the high intensity of the rainfall (Brito et al., 2016) are the  
47 key factors to rainfall disasters in mountainous regions in Brazil (Mello et al., 2020).

48 One of the regions most affected by rainfall disasters is the mountainous region of the  
49 Rio de Janeiro state (MRRJ) (Brasil, 2012; Freitas et al., 2012; Oliveira et al., 2016). In  
50 January/2011, landslides were triggered by extreme rainfalls, causing the so-called “mega-  
51 disaster” in this region. A total of 23 municipalities were affected, and seven of these were  
52 declared in a emergency situation (Cardozo and Monteiro, 2019). Petrópolis, Teresópolis, and  
53 Nova Friburgo municipalities recorded the highest number of victims. The most significant  
54 impacts in Nova Friburgo occurred in the urban area, whereas the rural areas were the most  
55 affected in the other two municipalities (Busch and Amorim, 2011; Cardozo and Monteiro,  
56 2019). Official reports indicated 918 fatalities, 22,604 displaced, and 8,795 homeless across  
57 the region (Freitas et al., 2012). This event was the worst natural disaster in Brazil’s history  
58 (Cardozo and Monteiro, 2019).

59 Some authors have assessed the efficiency of the early warning system (EWS) indexes  
60 in reducing risks from rainfall. However, due to the difficulty in obtaining and combine all the  
61 variables involved with landslides in an index that can be used as an early warning, indexes  
62 have been applied focusing on the extreme rainfall and the human and material damages (Xu  
63 et al., 2014; Calvello et al., 2015; Oliveira et al., 2016). Some indexes have been widely used  
64 in Brazil and the world, such as the accumulated rainfall in the last 24, 48, 72, and 96 hours,  
65 rainfall intensity ( $\text{mm h}^{-1}$ ), or even such variables evaluated simultaneously. Nevertheless,  
66 some of these indexes have shown to be inefficient. An example of this was the rainfall  
67 disasters in Campus do Jordão county in Serra da Mantiqueira (southeastern Brazil) in the  
68 year 2000. This event was caused by an accumulation of rain below the limit previously  
69 established in 72 hours (Mendes et al., 2018). Another example, it was the index used by the

70 *Alerta-Rio*, as 20 false alerts were issued for the four warning zones of the city between 2010  
71 and 2013.

72 Mello et al. (2020) proposed the use of  $R_{\text{day}}$  as a rainfall index as EWS for the Serra da  
73 Mantiqueira region (SMR), in Minas Gerais state (Southeast Brazil). Although this index has  
74 shown efficiency, it lacks a complementary spatial analysis using data from several stations  
75 with rain records every 15-minute, as they used data from only one station with this  
76 characteristic. This aspect makes it possible to better understand the genesis of extreme events  
77 in regions with a strong orographic influence, which the researchers did not properly  
78 characterize. In this direction, the purpose of this study is to fit a seasonal  $R_{\text{day}}$  model for the  
79 MRRJ. Based on this index, the main objective was to improve  $R_{\text{day}}$  as an index, which could  
80 be applied coupled with the EWS for rainfall disasters in this region in Brazil.

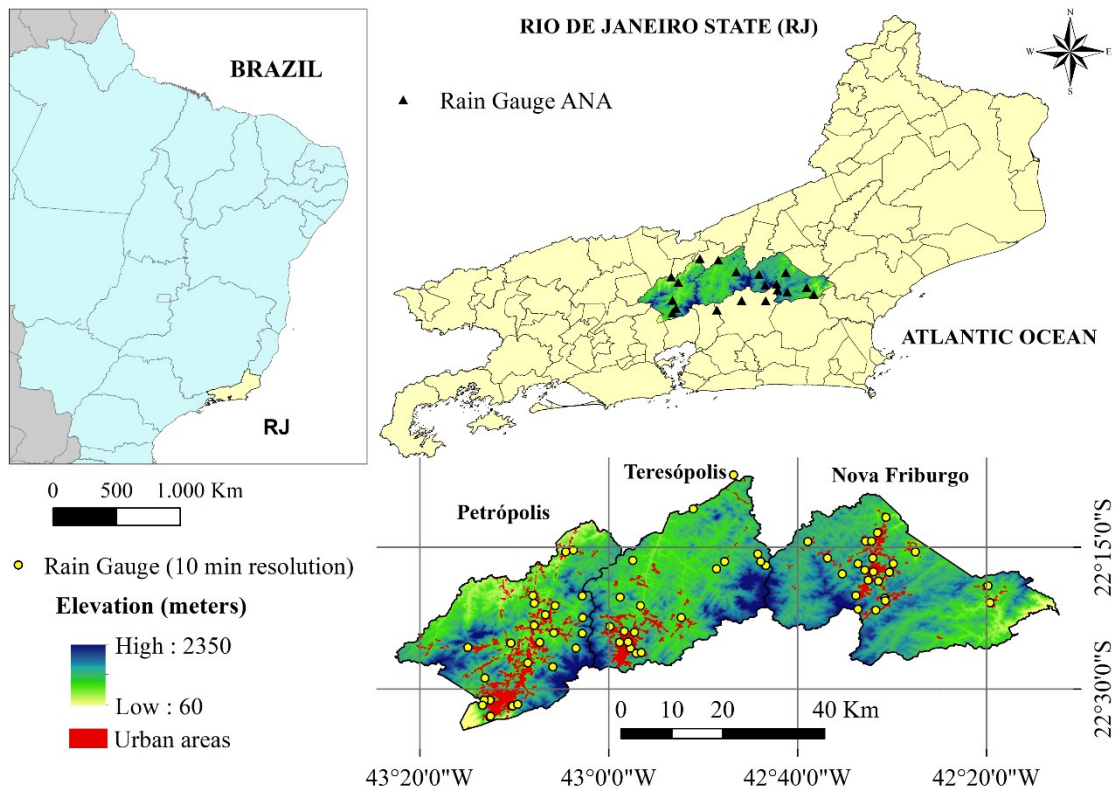
81

## 82 **2. MATERIAL AND METHODS**

### 83 **2.1 The mountainous region of Rio de Janeiro state (MRRJ)**

84 The MRRJ is located in Serra do Mar region, in southeast Brazil. In geomorphological  
85 terms, it is inserted in the Reverse Plateau unit (Garcia and Francisco, 2013), characterized by  
86 mountainous and steep relief, with altitudes ranging from 400 to 2350 meters (Figure 1). The  
87 predominant soils are the Cambisols, which are shallow, moderately permeable, with a high  
88 silt/clay ratio, low natural fertility, and with the formation of crusts that constraints the  
89 infiltration if the vegetation cover is scarce or absent (Pinto et al., 2018).

90 The geographical location of the three municipalities severely impacted by rainfall  
91 hazards is in Figure 1, as well as the location of the Brazilian National Water Agency (ANA)  
92 rain gauge stations and the National Center for Monitoring and Early Warning of Natural  
93 Disasters (CEMADEN) automatic rain gauges used in this study.



94

95 **Figure 1.** Geographical location of MRRJ, highlighting Nova Friburgo, Petrópolis, and  
 96 Teresópolis municipalities, the CEMADEN automatic rain gauges, and the ANA rain gauges.

97 The municipalities of Petrópolis (792 km<sup>2</sup>), Teresópolis (773 km<sup>2</sup>) and Nova Friburgo  
 98 (936 km<sup>2</sup>) were focused in this study because they are the most representative municipalities  
 99 in the population, and they were more prone to rainfall hazards in recent decades (Coelho  
 100 Netto et al., 2013). The population of these three municipalities is predominantly urban  
 101 (approximately 90%), totaling approximately 645,000 inhabitants (296,000, 166,000 and  
 102 183,000 in Petrópolis, Teresópolis, and Nova Friburgo, respectively) (IBGE, 2010; Coelho  
 103 Netto et al., 2013; Cardozo and Monteiro, 2019). Its economy is geared towards industry,  
 104 agriculture, and tourism (Coelho Netto et al., 2013).

105 The MRRJ climate is generally characterized as Cwb (according to the Köppen  
 106 climate classification), with dry winters and rainy summers. The annual average temperatures  
 107 are around 16°C (Coelho Netto et al., 2013) and the summer accounts for 70% of the rainfall  
 108 between October and March. The winters are cool and dry (Dourado et al., 2012). The rainfall

109 pattern in the MRRJ is driven by frontal systems; convective rains in the summer; South  
 110 Atlantic Convergence Zone (SACZ); orographic effects; tropical and subtropical cyclones;  
 111 surface water temperature of the Subtropical Atlantic Ocean; and maritimity (Reboita et al.,  
 112 2010).

113 Nova Friburgo has been hit by the highest rainfall amount throughout the state of Rio  
 114 de Janeiro, with an annual average of 2,500 mm in the highest areas, decreasing progressively  
 115 towards the north (N) as the altitudes decrease (Coelho Netto et al., 2013; Cardozo and  
 116 Monteiro, 2019). The average annual rainfall in Teresópolis also varies in the North-South  
 117 direction (from 2200 to 1500 mm), and in Petrópolis (from 1900 to 1000 mm). The rainiest  
 118 period occurs between December and February, when the monthly average rainfall varies  
 119 between 340 and 240 mm in the highest altitudes in the southern MRRJ, and between 240 and  
 120 150 mm in the northern (Coelho Netto et al., 2013).

121

## 122 **2.2 Rainfall erosivity calculation (EI<sub>30</sub>)**

123 Datasets of rainfall from 68 automatic rain gauges provided by CEMADEN with a 10-  
 124 minute temporal resolution (Figure 1) were used to calculate EI<sub>30</sub>, using the available period  
 125 between 2014 and 2020. The following equations were used to calculate EI<sub>30</sub>:

$$126 \quad ke_d = 0.29 \cdot [1 - 0.72 \cdot \exp(-0.082 \cdot i_d)] \quad (1)$$

$$127 \quad E_d = Ke_d \cdot P_d \quad (2)$$

$$128 \quad KE = (\sum_{d=1}^n E_d) \quad (3)$$

$$129 \quad EI_{30} = KE \cdot I_{30} \quad (4)$$

130 Equation 1 allows calculating the kinetic energy per mm of rain ( $ke_d$ ) per time interval  
 131 “d” ( $\text{MJ}\cdot\text{ha}^{-1}\cdot\text{mm}^{-1}$ ), in which  $i_d$  is the rainfall intensity ( $\text{mm}\cdot\text{h}^{-1}$ ) (McGregor and Mutchler,  
 132 1976). In equation 2,  $E_d$  is the kinetic energy ( $\text{MJ}\cdot\text{ha}^{-1}$ ), and  $P_d$  is rainfall depth (mm), both in

133 the “d” time interval. Thus, the kinetic energy of the event is obtained by the sum of the  
 134 kinetic energy ( $E_d$ ) calculated for each time interval ( $KE$ , MJ.ha<sup>-1</sup>) (Equation 3), where “n”  
 135 corresponds to the number of the time interval “d”. Finally, the  $EI_{30}$  calculation for the event  
 136 (MJ.ha<sup>-1</sup>.mm.h<sup>-1</sup>) (Equation 4) is made by multiplying  $KE$  by the 30-minute maximum rainfall  
 137 intensity ( $I_{30}$ ) (mm.h<sup>-1</sup>).

138 Two conditions were considered to separate individual erosive events:  $KE > 3.6$   
 139 MJ.ha<sup>-1</sup> (De Maria, 1994); and  $I_{30} \geq 13.3$  mm.h<sup>-1</sup> (Xie et al., 2002). Nevertheless,  $EI_{30}$  is not  
 140 necessarily synonymous with  $R_{day}$ , since a single rain event can have a duration greater than  
 141 one day, or more than one erosive event may occur on the same day. Therefore, three  
 142 situations are possible to define  $R_{day}$  (Xie et al., 2016; Mello et al., 2020):

143 Type I: a day with only one rain event ( $R_{day} = EI_{30}$  of the event);

144 Type II: a day with multiple rain events separated by  $> 6$  hours ( $R_{day} =$  sum of the  $EI_{30}$   
 145 of each event in the day); and

146 Type III: a day with rainfall event that lasts over 24 hours ( $R_{day} = KE$  considering the  
 147 24-hour interval with the highest total rainfall multiplied by the highest  $I_{30}$  for their  
 148 calculation).

149

### 150 **2.3 Seasonal model for estimating $R_{day}$**

151 A seasonal  $R_{day}$  model was fitted based on the study by Yu and Rosewell (1996):

$$152 \quad R_{day} = \alpha \cdot [1 + \eta \cos(2\pi f j - \omega)] \cdot P_{day}^{\beta} \quad (5)$$

153

154 In which  $j$  is the fortnight of the year (ranging from 1 to 24);  $f = 1/24$ ;  $\eta$ ,  $\alpha$ ,  $\omega$  and  $\beta$  are  
 155 the fitted parameters. The  $\eta$  parameter is related to the amplitude in the variation of the  $\alpha$   
 156 parameter;  $\omega$  is the parameter related to the fortnight with the highest accumulated rainfall  
 157 erosivity;  $\beta$  is a parameter considered for modeling the non-linearity of daily rainfall and

158 respective erosivity (Richardson et al. 1983). In the MRRJ, the first half of January has the  
 159 highest accumulated total erosivity (based on seven years of recording);  $\omega = \pi/6$ .

160 The model parameters were estimated using the least squares method considering the  
 161  $R_{\text{day}}$  and the respective daily rainfall observed in the 68 automatic rain gauges. For this, we  
 162 split the dataset (rainfall erosive events) into two groups: one for fitting the daily rainfall  
 163 erosivity model (equation 5) and the other for analyzing the model's performance. For the  
 164 latter, approximately 37% of the data were used, being randomly chosen according to the  
 165 number of erosive events distributed in daily rainfall classes (< 15 mm; 16-20 mm; 21-30; 31-  
 166 40 mm; 41-50 mm; 51-75 mm; 76-100; > 101 mm).

167 Two precision statistics were adopted (Angulo-Martinez and Beguería, 2009):

168 i) Nash-Sutcliffe Efficiency Coefficient ( $C_{NS}$ ) (Nash and Sutcliffe, 1970):

169

$$170 \quad C_{NS} = 1 - \frac{\sum_{i=1}^N (E_{oi} - E_{ei})^2}{\sum_{i=1}^N (E_{oi} - \bar{E}_o)^2} \quad (6)$$

171 ii)  $P_{\text{bias}}$  that measures the trend of estimates, and is calculated by:

$$172 \quad P_{\text{bias}} = \frac{\sum_{i=1}^N (E_{oi} - E_{ei})}{N} \quad (7)$$

173

## 174 **2.4 Natural disaster rainfall-based alert indexes**

### 175 **2.4.1 Previous rainfall indexes**

176 Brooks and Stensrud (2000) defined that a rainfall event is classified as intense when  
 177 the precipitation intensity is  $\geq 25.4$  mm/h. Groisman et al. (2001) established that intense and  
 178 very intense rainfall can be separated using a fixed threshold of 50.8 and 101.6 mm/day,  
 179 respectively, or the values corresponding to the 90<sup>th</sup> and 99<sup>th</sup> percentiles. In investigating the  
 180 occurrence of extreme events in the United States, Groisman et al. (2012) considered four  
 181 classes of precipitation: moderately intense (12.7-25.4 mm/day), intense (25.4-76.2 mm/day),



182 very intense (76.2-154.9 mm/day), and extreme intense ( $> 154.9$  mm/day); the latter is related  
183 to floods, property damage, accidents, and fatalities.

184 Dolif and Nobre (2012) defined an extreme event for the city of Rio de Janeiro as one  
185 that causes a precipitated accumulation  $> 50$  mm in any interval of 24 hours. This threshold is  
186 the one used by the World Meteorological Organization (WMO) in the “Severe Weather  
187 Information Centre” (<http://severe.worldweather.org/rain/>), applied in intense precipitation  
188 prediction models (Pristo et al., 2018). Still, regarding the city of Rio de Janeiro, a system  
189 called *Alerta-Rio* has been applied since April/2010. However, despite its good performance  
190 in predicting extreme events and alerting the population to these, its implementation cost is  
191 high since it is based on rain intensity data derived from meteorological radars.

192 Despite the difficulty of establishing a single value as an alert index, it is known that  
193 precipitation is one of the factors that most triggers natural disasters (Guzzetti et al., 2007). In  
194 addition, the forecast of this variable can be made 48 or even 72 hours in advance (Oliveira et  
195 al., 2016), providing enough time for the authorities to assess the event and warn the  
196 population of imminent risks. Thus, precipitation has been used to compose the majority of  
197 EWS.

198

#### 199 **2.4.2 Application of the $R_{\text{day}}$ as an EWS**

200  $R_{\text{day}}$  thresholds are proposed as an index to be used in the EWS. These thresholds were  
201 established through the joint analysis of the  $R_{\text{day}}$  values, which concomitantly caused rainfall  
202 hazards with the respective consequences observed in eight events that hit the MRRJ in the  
203 last two decades.

204 Maximum daily rainfall erosivity ( $R_{\text{maxday}}$ ) (Mello et al., 2020) map was developed to  
205 identify areas more vulnerable to rainfall hazards. It is based on the maximum daily rainfall  
206 observed in at least 22 years since it is the minimum period to characterize the rainfall

207 erosivity pattern for a given region (Wischmeier and Smith, 1978). Its mapping was  
208 developed by means kriging techniques, considering the highest rainfall values observed in  
209 the MRRJ in the last three decades (1990-2019).

210 The  $R_{\text{day}}$  index definition is based on (Mello et al., 2020): i) detailed survey of the  
211 events which caused natural disasters, characterizing, in this order, fatalities, homeless, and  
212 damage in the infrastructure; ii) other indexes were used for comparative purposes when  
213 establishing  $R_{\text{day}}$  thresholds. Thus,  $R_{\text{day}}$  intervals were proposed for MRRJ according to the  
214 occurrences and the respective  $R_{\text{day}}$ , linking these intervals to the consequences registered,  
215 and comparing them with other existing indexes.

216 The indexes used in this study for comparison purposes are those used by *Alerta-Rio*,  
217 operated by the Geotechnical Foundation of the municipality of Rio de Janeiro (*GEO-Rio*),  
218 and those presented by Oliveira et al. (2016), who studied the precipitation thresholds that  
219 caused rainfall hazards in the Nova Friburgo municipality (Table 1). The established indexes  
220 can be based on a relationship between rainfall and landslides or through statistical analysis  
221 (Calvello et al., 2015). The intervals that consider a period of 24 and 72 hours is presented in  
222 Table 1. Both indexes consider the rainfall duration; Alerta Rio one hour, 24 hours, and 72  
223 hours, while Oliveira et al. (2006) 24 hours, 48 hours, and 72 hours. Besides, both indexes  
224 proposed a classification warning according to the magnitude of the rain; Alerta Rio defined  
225 “Mean,” “High,” and “Very High” warning, linking them to the respective duration and an  
226 interval of the rainfall depth. Oliveira et al. (2006) created three levels, A, B, and C, which are  
227 associated with the respective duration and rainfall depth. Similar to Alerta Rio, these levels  
228 indicate the concern with the rainfall impact, increasing from A to C.

229 **Table 1.** *Precipitation limits currently adopted as warning indexes in Rio de Janeiro state.*

Duration (hours)	Alert level according to accumulated rainfall (mm) – Alerta Rio		
	Mean	High	Very high
1	25-50	50-80	>80
24	85-140	140-220	>220
72	140-220	220-300	>300

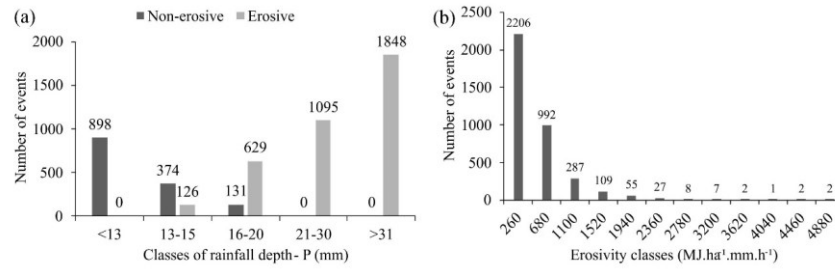
Criteria	Accumulated rainfall (mm) (Oliveira et al. 2016)		
	24h	48h	72h
A	50	60	100
B	50	75	120
C	75	120	150

230

231 **3. RESULTS**232 **3.1 Daily rainfall erosivity modeling in the MRRJ**

233 Based on 68 CEMADEN stations, 5,101 rainfall events with  $I_{30} \geq 13.3 \text{ mm.h}^{-1}$  (the  
234 first step for split rainfall erosivity events) were identified between 2014 and 2019 in MRRJ,  
235 with the lowest observed amount of 6.7 mm. However, some of these events are not erosive  
236 according to the kinetic energy ( $KE > 3.6 \text{ MJ ha}^{-1}$ ). Therefore, the second step consisted of  
237 separating those that are erosive. From the 5,101 events, 3,698 were classified as erosive  
238 events, i.e.,  $KE > 3.6 \text{ MJ.ha}^{-1}$ , corresponding to 72.5% of the studied events. The number of  
239 erosive and non-erosive events and the frequency and respective class of  $R_{\text{day}}$  in MRRJ are  
240 presented, respectively, in Figures 2(a) and (b).

241



242  
 243 **Figure 2.** The number of erosive and non-erosive events (2014 to 2019) per rainfall classes  
 244 (a) and frequency of  $R_{\text{day}}$  observed in MRRJ (b).

245 Table 2 shows the number and percentage of erosive events, the percentage of  
 246 observed erosivity, and the average  $I_{30}$  ( $\text{mm.h}^{-1}$ ) for each rainfall class.

247

248 **Table 2.** Percentage of erosive events and total erosivity for different rainfall classes.

Rainfall		% of accumulated $EI_{30}$		Average $I_{30}$
(mm)	N <sup>o</sup> . of events	% of Events	( $\text{MJ.ha}^{-1}.\text{mm.h}^{-1}$ )	( $\text{mm.h}^{-1}$ )
<15	126	3.4	0.5	26.1
16-20	629	17.0	5.2	25.6
21-30	1095	29.6	15.7	29.0
31-40	679	18.4	16.1	34.5
41-50	428	11.6	14.9	39.6
51-75	497	13.4	24.3	42.5
76-100	125	3.4	10.2	45.6
>101	119	3.2	13.1	46.2

249

250 The classification of erosive events in terms of their type is: 83% Type I; 11.6% Type  
 251 II; and 5.4% Type III.

252 To apply the  $R_{\text{day}}$  model, it is fundamental to establish a minimum daily rainfall that  
 253 potentially can triggers a rainfall erosive event. Figure 2a shows that all 898 events < 13 mm  
 254 were not classified as erosive. However, 126 events in the 13 - 15 mm interval (25.2%) were

255 erosive, which allows us to infer that the minimum precipitation depth to be considered  
 256 erosive is within this interval, bearing in mind that some 13 mm events were erosives.

257 Erosive events had the following characteristics: i) they are generated by rainfall  $\geq 13$   
 258 mm; ii) all rainfall events  $\geq 22$  mm are erosive; iii) approximately half of the erosive events  
 259 (1848 out of 3698 events) occur for rainfall  $\geq 31$  mm; and iv) despite representing  
 260 approximately 50% of the total number of erosive events, rainfall  $\geq 31$  mm corresponds to  
 261 78.6% of the total observed rainfall erosivity over MRRJ.

### 262 3.2 Seasonal $R_{day}$ model for MRRJ

263 The fitted seasonal model for MRRJ presented the following structure:

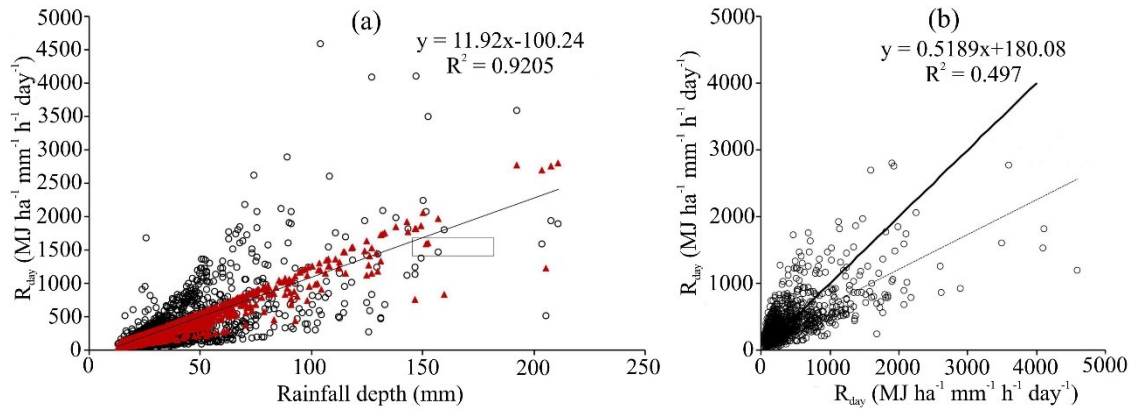
$$264 R_{day} = 3.3888 \cdot \left[ 1 + 0.4659 \cdot \cos\left(\frac{2 \cdot \pi \cdot j}{24} - \frac{\pi}{6}\right) \right] \cdot P_{day}^{1.2028} \quad (8)$$

265 This model describes the inter-daily annual seasonality of  $R_{day}$  by estimating the  
 266 parameters “ $\alpha$ ”, “ $\eta$ ” and “ $\beta$ ” (3.3888; 0.4659; 1.2028; respectively). An important detail is  
 267 that the fitted parameters spatially represent the MRRJ since it was determined based on data  
 268 from 68 rain gauge stations with precipitation data recorded every 10 minutes.

269 The precision statistics associated with calibration ( $C_{NS} = 0.51$ ;  $P_{bias} = -0.56$ ) and  
 270 validation ( $C_{NS} = 0.50$ ;  $P_{bias} = -2.22$ ) demonstrate satisfactory results for the  $R_{day}$  model,  
 271 especially when considering that this estimate is made based only on daily rainfall and the  
 272 period of the year.

273 Figures 3a and 3b represent the fitted model applied to the events (1,368 events)  
 274 separated exclusively for validation. The regression in Figure 3a means a relationship between  
 275 estimated  $R_{day}$  values by the fitted model in function of rainfall depth (red triangles). Through  
 276 this fitting, one can observe that the model could capture the seasonality effect on daily  
 277 rainfall erosivity, i.e., different  $R_{day}$  values were estimated with the same precipitation depth,  
 278 meaning that these events occurred in different seasons of the year.

279 In Figure 3b, it is possible to verify that the estimated  $R_{\text{day}}$  values fitted reasonably  
 280 well to the observed ones. However, overestimation and understation values can be seen,  
 281 respectively, for the lowest and the highest values.

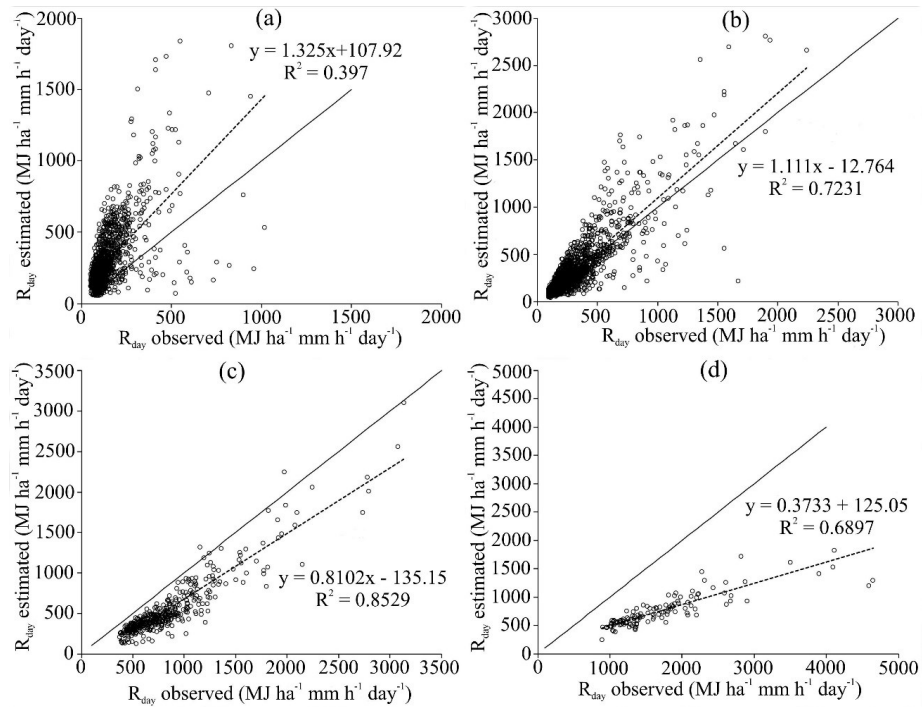


282

283 **Figure 3.** Behavior of the  $R_{\text{day}}$  by the seasonal model applied to the validation data.

284

285 Figure 4 shows the model fitting graphs for MRRJ considering different classes of  $I_{30}$ .  
 286 It can be seen in Figure 4a that the model tends to overestimate  $R_{\text{day}}$  for  $I_{30} < 25$  mm.h<sup>-1</sup>. On  
 287 the other hand, the model's performance is superior for the  $I_{30}$  between 25 and 50 mm.h<sup>-1</sup>  
 288 (Figure 4b), and between 51 and 75 mm.h<sup>-1</sup> (Figure 4c), with good precision. However, the  
 289 model underestimates  $R_{\text{day}}$  for the greatest  $I_{30}$  class (Figure 4d).

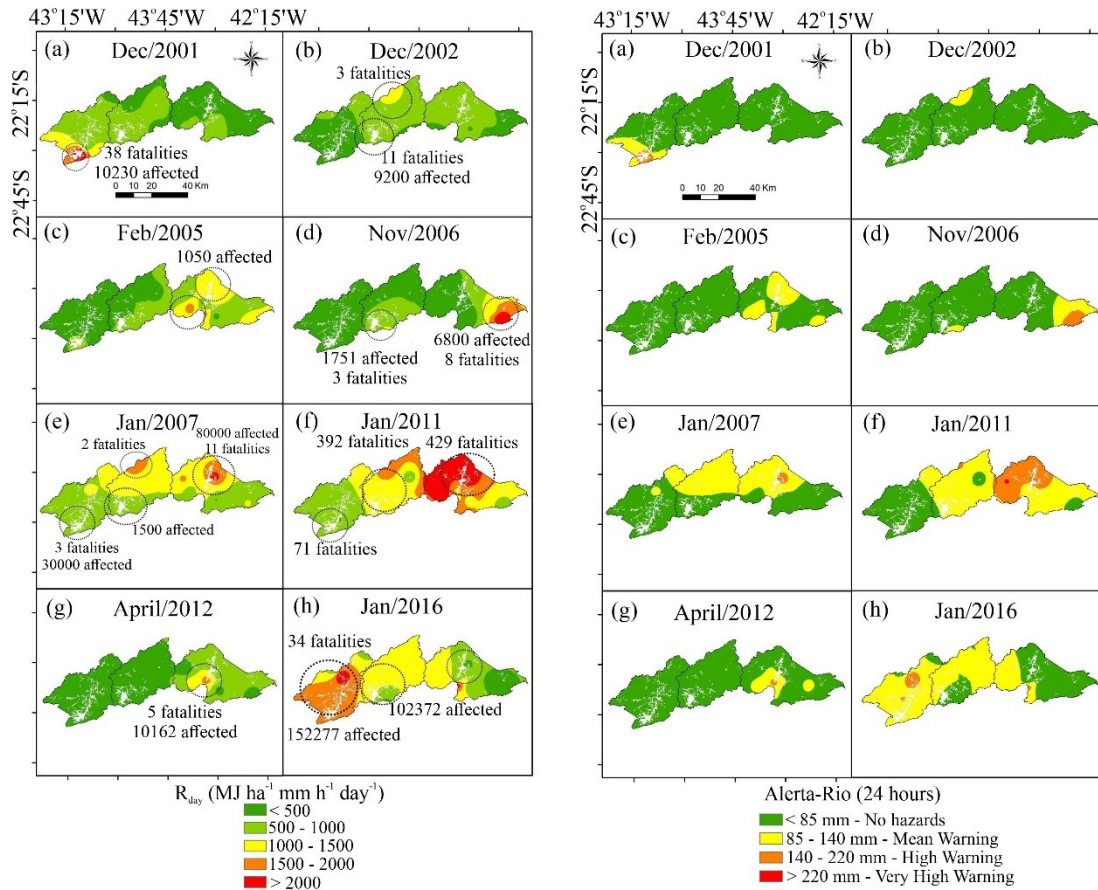


290

291 **Figure 4.** Model fitting for different  $I_{30}$  classes (a.  $I_{30} < 25$ ; b.  $25 \leq I_{30} \leq 50$ ; c.  $51 \leq I_{30} \leq 75$ ;  
 292 and d.  $I_{30} > 75$ ).

### 293 3.3 Relation between $R_{day}$ and rainfall hazards in MRRJ

294 To relate  $R_{day}$  values and the most significant rainfall hazards provoked by rainfall in  
 295 MRRJ, maps of it were developed (Figure 5 – left column). For comparing purposes, a map  
 296 using the EWS developed by *Alerta-Rio* was also developed (Figure 5 – right column), which  
 297 allows observing how  $R_{day}$  is more sensitive and complete than the previous alert index.



298

299 **Figure 5.** Maps of the most severe rainfall hazards in MRRJ (see Table 3) and respective  $R_{day}$   
 300 values (maps in left column) and using *Alerta-Rio* (maps in right column).

301

302 All three municipalities had  $R_{day} > 1,500$  MJ.ha<sup>-1</sup>.mm.h<sup>-1</sup>.day<sup>-1</sup> at some point, and  
 303 these events have always been linked to disasters that culminated in thousands of people  
 304 affected (fatalities, displaced, homeless, injured people), as further depicted in Table 3. This  
 305 table has as purpose of presenting the most impacting rainfall hazards in MRRJ between 2001  
 306 and 2016, respective impacts and risk classification (EWS) according to *Alerta-Rio*, taking the  
 307 greatest precipitation in 24 hours or 72 hours, i.e., the worst situation (Table 1). Also, the  
 308 disasters were presented according to the most affected (urban or rural), and the respective  
 309  $R_{day}$  was calculated using the fitted model.

310

311

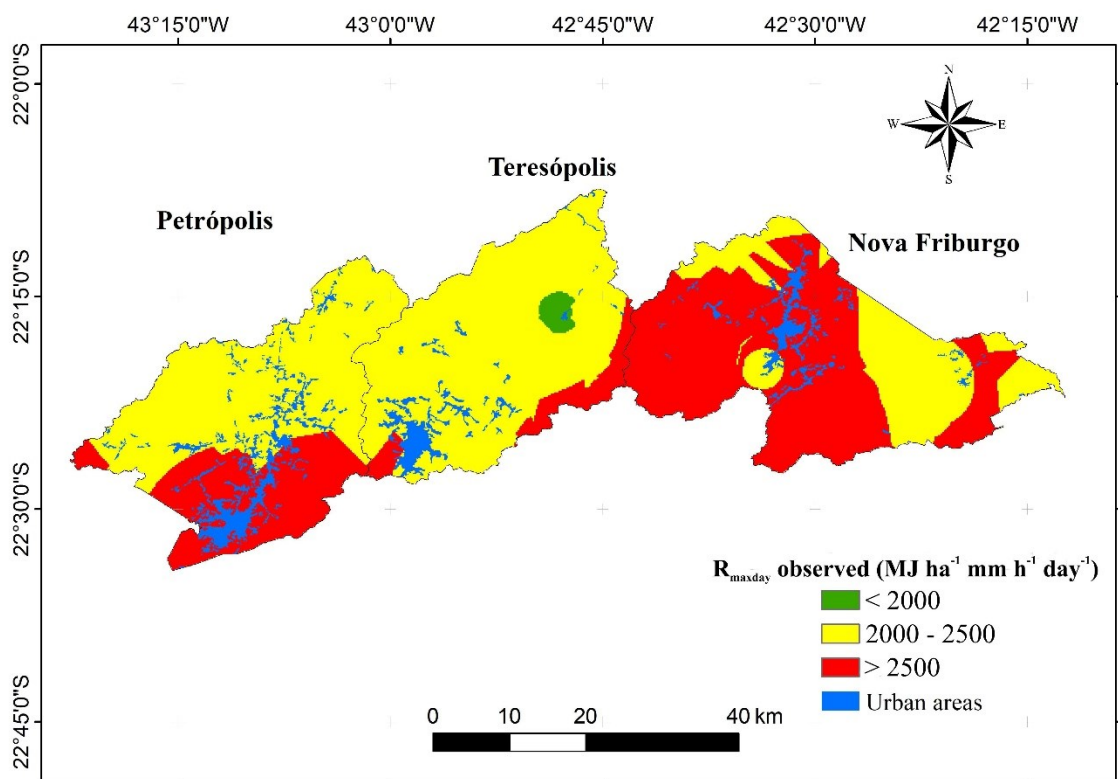


312 **Table 3.** Summary of the rainfall hazards observed in the MRRJ in the last two decades and respective estimated  $R_{day}$ .

Date (DD/MM/Year)	Municipality	Displaced	Fatalities	Number of affected	$R_{day}$ (MJ ha <sup>-1</sup> mm.h <sup>-1</sup> day <sup>-1</sup> )	Area**	P24(mm)	P72(mm)	Alerta-Rio
24/12/2001	Petrópolis	5017	38	10230	3125.4	Urban	220.1	220.1	Very high
18/12/2002	Teresópolis	253	14	9200	1293.5	Rural	105.7	171.6	Mean
04/02/2005	Nova Friburgo	249	0	1050	1788.9	Rural	134.6	170	Mean
29/11/2006	Teresópolis	248	3	1751	1198.7	Urban	110.5	169.6	Mean
29/11/2006	Nova Friburgo	545	8	6800	2578.2	Rural	208.8	223	High
04/01/2007	Petrópolis	525	3	30000	1133.9	Rural	92.2	163.6	Mean
04/01/2007	Nova Friburgo	4196	11	80000	2238.4	Rural	162.3	395.9	High
04/01/2007	Teresópolis	229	2	1500	1851.3	Rural	138.6	160.1	Mean
12/01/2011	Petrópolis	7144	71	*	900.1	Rural	76.1	80.3	No hazards
12/01/2011	Nova Friburgo	5317	429	*	2594.6	Urban	183.5	201.8	High
12/01/2011	Teresópolis	15837	392	*	1962.8	Rural	145.5	249.8	High
06/04/2012	Nova Friburgo	2371	5	10162	1875.1	Urban	173	176.5	High
15/01/2016	Petrópolis	523	34	152277	1682.4	Urban	128.2	221.4	Mean
15/01/2016	Teresópolis	144	0	102372	1016.7	Rural	84.2	130.5	No hazards

313 \* Official sources did not account for an approximate number per municipality, but it is known that more than 1,000,000 people were affected across the region. \*\* Areas more  
314 impacted (urban and rural).

315 The  $R_{\text{day}}$  estimates can be useful to analyze whether a given region can be hit by  $R_{\text{day}}$   
 316 that causes rainfall hazards. In addition, the development of  $R_{\text{maxday}}$  maps can be used as a tool  
 317 to identify the most vulnerable areas to rainfall hazards. These maps can also be helpful in  
 318 planning and managing the reduction of impacts caused by very erosive rains, which occur in  
 319 mountainous regions of southeastern Brazil. The spatial distribution of  $R_{\text{maxday}}$  in MRRJ is  
 320 presented in Figure 6 and was prepared using the maximum daily precipitation observed in  
 321 the last 30 years (1990-2019).



322  
 323 **Figure 6.**  $R_{\text{maxday}}$  mapping for the MRRJ considering the last three decades.

324  
 325 The highest  $R_{\text{maxday}}$  values ( $\geq 2,500$  MJ.ha<sup>-1</sup>.mm.h<sup>-1</sup>.day<sup>-1</sup>) were estimated in southern  
 326 Petrópolis, eastern Teresópolis, and the largest part of the Nova Friburgo, matching with the  
 327 highest altitudes. The urban areas of Petrópolis and Nova Friburgo are inserted in these  
 328 regions, and Teresópolis is in a region where  $2,000 < R_{\text{maxday}} < 2,500$  MJ.ha<sup>-1</sup>.mm.h<sup>-1</sup>.day<sup>-1</sup>.  
 329 These high values are explained based on the combination of the effects of orographic rainfall

330 events due to altitude and proximity to the Atlantic Ocean. Therefore, these are the most  
331 vulnerable areas to rainfall hazards in MRRJ.

332 Nova Friburgo is the municipality with the highest  $R_{\text{maxday}}$  values. Thus, it is the most  
333 vulnerable to fatalities, damage to infrastructure, economy, and society in general. On the  
334 other hand, it is observed that practically all of the MRRJ presented  $R_{\text{maxday}}$  values  $> 2,000$   
335  $\text{MJ}\cdot\text{ha}^{-1}\cdot\text{mm}\cdot\text{h}^{-1}\cdot\text{day}^{-1}$ , which is higher than the previously established index ( $1,500 \text{ MJ}\cdot\text{ha}^{-1}\cdot\text{mm}\cdot\text{h}^{-1}\cdot\text{day}^{-1}$ ), allowing classifying this region as very vulnerable to fatalities, homelessness,  
336 and infrastructure damages.  
337

338

## 339 4. DISCUSSION

### 340 4.1 General aspects of $R_{\text{day}}$ in MRRJ

341 Despite the lower frequency of erosive events in the last three precipitation classes  
342 (Table 2;  $P \geq 51 \text{ mm}$ ), these are the most expressive events in terms of erosivity, representing  
343 47.6% of the total rainfall erosivity for the region. This fact demonstrates that only an erosive  
344 rain event can easily trigger natural disasters in the region. Thus, the study of these events is  
345 essential for analyzing the occurrence of natural disasters and a more practical index for  
346 issuing warning signs for natural disasters.

347 In MRRJ, there is a predominance of type I events due to the fact that the Serra do  
348 Mar is close to the Atlantic Ocean, increasing the presence of air humidity, leading to  
349 orographic and convective rains, which are generally of short to medium duration. Mello et al.  
350 (2020) for Mantiqueira Range region, southeast Brazil, also observed the dominance of type I,  
351 which is linked with the pattern of rainfall in tropical regions in summer. Most erosive events  
352 are associated with convective rains, characterized as local events of short duration and high  
353 intensity, increasing the  $KE$  values, as well as the maximum values for  $I_{30}$ . These rains are  
354 common in the summer, justifying the predominance of Type I. Despite the high magnitude of

355 the total precipitation, events classified as Type III generally present lower  $I_{30}$  values since  
356 they come from high-duration frontal systems and less intensity than convective rains.  
357 However, several rainfall hazards are associated with this type of event since they are  
358 responsible for soil saturation, increasing the susceptibility to landslides and floods. It is also  
359 known that the variability in precipitation intensity during these frontal events is small, so that  
360 Type III events do not tend to overestimate  $R_{day}$  even with a higher amount of precipitation  
361 (Xie et al., 2016). Also, the South Atlantic Convergence Zone (SACZ) can hit the Southeast  
362 Brazil in summer, being responsible for several consecutive rainy days, and can therefore be  
363 highlighted as a potential source for types II and III.

364 Because a rainfall of 13 mm generated some erosive rains, this value is considered  
365 more appropriate as a threshold for erosive rainfall in MRRJ. This value is similar to those  
366 suggested by Xie et al. (2002), who conducted a study to characterize the erosive thresholds  
367 of the rains (from 11.9 to 12.8 mm), as well as Xie et al. (2016), who considered 12.0 mm as  
368 the most appropriate for eastern China, and Wischmeier & Smith (1978) suggested 12.7 mm  
369 for the United States. Mello et al. (2020) observed that none of the studied events smaller than  
370 12 mm was erosive, while some events with precipitation equal to 13 mm were classified as  
371 erosive in the Mantiqueira Range region.

372

#### 373 **4.2 Seasonal $R_{day}$ model for MRRJ**

374 Mello et al. (2020) fitted values of “ $\alpha$ ”, “ $\eta$ ” and “ $\beta$ ” for Mantiqueira range region  
375 equal to 1.8524, 0.2827, and 1.2950, respectively. Comparing these values with those fitted  
376 for the MRRJ, it seems that the “ $\alpha$ ” parameter, which is responsible for the  $R_{day}$  annual  
377 variation, is intrinsic to each region and did not show any similarity. “ $\beta$ ” models the non-  
378 linearity variation between rainfall and rainfall erosivity (Yang and Yu, 2015; Wang et al.,  
379 2017), and therefore the value for MRRJ is similar to that for Mantiqueira range region. It is

380 directly related to the rainfall patterns. Finally, “ $\eta$ ” is the parameter that models the amplitude  
381 of the interannual variation of “ $\alpha$ ” and is not similar to the value for the Mantiqueira range  
382 region. Yu and Rosewell (1996) and Xie et al. (2016) fitted this model for eastern China and  
383 Australia, respectively, and found values equal to 0.2686, 0.5412 and 1.7265; and 0.535,  
384 0.306 and 1.46 for “ $\alpha$ ”, “ $\eta$ ” and “ $\beta$ ”, respectively, as mean parameters of the respective  
385 studied regions. Wang et al. (2017) also fitted a similar model in a subtropical region of China  
386 and found “ $\alpha$ ” varying from 1.04 to 3.12, “ $\eta$ ” from 0.13 to 0.74, and “ $\beta$ ” from 1.16 to 1.46.  
387 Therefore, it is recommended that each geographical region has its own fitted model since the  
388 parameters are associated with the respective rainfall pattern.

389 The behavior of the fitted model for MRRJ is similar to those found by Xie et al.  
390 (2016) and Mello et al. (2020), who found that this model shows an overestimation behavior  
391 for the lowest  $R_{\text{day}}$  values and produces better results for more intense rainfall events, which  
392 generate higher erosivity values. Despite the similarity of the results, Xie et al. (2016) and  
393 Mello et al. (2020) did not relate the model’s performance to  $I_{30}$  behavior. In general, the  
394 model fits reasonably well to MRRJ, since the predominant  $I_{30}$  class in the region is 25 - 75  
395  $\text{mm h}^{-1}$  (Figure 4).

396

### 397 **4.3 $R_{\text{day}}$ and rainfall hazards in MRRJ: application of $R_{\text{day}}$ and comparison with** 398 **previous indexes**

399 In this section, it is highlighted the main impacts of the rainfall hazards and respective  
400  $R_{\text{day}}$ , which enable us to propose thresholds for  $R_{\text{day}}$  in MRRJ (Table 3), and to compare it  
401 with the previous existent. Petrópolis county was hit by a rainfall event in 2001 (220.1 mm in  
402 24 hours) impacting the urban area, causing 38 fatalities ( $R_{\text{day}} > 3,000 \text{ MJ ha}^{-1} \text{ mm h}^{-1} \text{ day}^{-1}$ ).  
403 Similarly, the Teresópolis county was hit by rainfall in 2002 that resulted in  $R_{\text{day}}$  ranging from  
404 500 to 1,000  $\text{MJ} \cdot \text{ha}^{-1} \cdot \text{mm} \cdot \text{h}^{-1} \cdot \text{day}^{-1}$  in most part of its area. These events led to 11 fatalities and

405 more than 9200 habitants affected. In the northern area,  $R_{\text{day}}$  reached  $1,500 \text{ MJ}\cdot\text{ha}^{-1}\cdot\text{mm}\cdot\text{h}^{-1}\cdot\text{day}^{-1}$   
406  $^1\cdot\text{day}^{-1}$  and caused people to be buried by landslides. The  $R_{\text{day}}$  values in the urban area of  
407 Nova Friburgo in 2005 ranged from 500 to  $1,500 \text{ MJ}\cdot\text{ha}^{-1}\cdot\text{mm}\cdot\text{h}^{-1}\cdot\text{day}^{-1}$  affecting 1050  
408 inhabitants, and leaving 249 homeless. The  $R_{\text{day}}$  values in the rural area were between 1,500  
409 and  $2,000 \text{ MJ}\cdot\text{ha}^{-1}\cdot\text{mm}\cdot\text{h}^{-1}\cdot\text{day}^{-1}$ . The municipalities of Nova Friburgo (545 homeless and eight  
410 fatalities), and Teresópolis (with 248 homeless and three fatalities) were severely affected  
411 again in 2006. In this year, the  $R_{\text{day}}$  values covered all the classes, with the highest values  $>$   
412  $2,000 \text{ MJ}\cdot\text{ha}^{-1}\cdot\text{mm}\cdot\text{h}^{-1}\cdot\text{day}^{-1}$ . The years of 2007 and 2011 had the highest  $R_{\text{day}}$  values and the  
413 greatest spatial coverage, resulting in 16 fatalities and 111,500 inhabitants affected.

414 The rainfall disaster that occurred in 2011 deserves special attention, since it was the  
415 worst observed in Brazil (Cardozo and Monteiro, 2019). This disaster not only caused a high  
416 number of fatalities, but also significant economic losses and damages. Petrópolis,  
417 Teresópolis and Nova Friburgo recorded the highest number of victims in MRRJ. The greatest  
418 impact in Nova Friburgo was observed predominantly in the urban area, while in the other  
419 two municipalities were on the rural areas (Busch and Amorim, 2011; Cardozo and Monteiro,  
420 2019). The  $R_{\text{day}}$  values in Nova Friburgo exceeded  $2,500 \text{ MJ}\cdot\text{ha}^{-1}\cdot\text{mm}\cdot\text{h}^{-1}\cdot\text{day}^{-1}$ , and the entire  
421 urban area presented values varying from 1,500 to  $> 2,000 \text{ MJ}\cdot\text{ha}^{-1}\cdot\text{mm}\cdot\text{h}^{-1}\cdot\text{day}^{-1}$ , which  
422 resulted in 434 fatalities (47% overall) (Cardozo et al., 2017, 2018; Cardozo and Monteiro,  
423 2019). On the same day, the total number of homeless in Teresópolis reached 15,837  
424 inhabitants, and it is estimated that more than 1 million people were affected in the three  
425 municipalities.

426 Nova Friburgo was again affected by similar natural disasters in 2012, however, unlike  
427 in 2011, they impacted the region in a more isolated way.  $R_{\text{day}}$  values ranged from 500 to  
428  $2,000 \text{ MJ}\cdot\text{ha}^{-1}\cdot\text{mm}\cdot\text{h}^{-1}\cdot\text{day}^{-1}$ , resulting in five fatalities, 2,371 homeless and more than 10,000  
429 affected inhabitants. In analyzing the year 2016 (Figure 5), it is observed that there was a

430 considerable spatial range of the  $R_{\text{day}}$  values, with emphasis on the municipality of Petrópolis  
431 (34 fatalities, 523 displaced people, and 152,277 inhabitants affected). The fact that the  
432 number of victims decreased after the 2011 disaster compared to the number of victims in the  
433 years 2012 and 2016 indicates that the public policies, mainly the creation of structures such  
434 as CEMADEN, the Technical Support and Emergency Task Force at the National Secretariat  
435 for Civil Defense and the National Force of Brazilian Health System (SUS) had a positive  
436 effect on the protocols associated with natural disaster management.

437         Based on these data, it is possible to suggest some thresholds and possible impacts  
438 related to them. However, such thresholds do not necessarily mean that impacts, especially  
439 fatalities, may occur, since the system for protecting the population from these events is  
440 currently more structured than in the past. Therefore, we have: (i)  $R_{\text{day}} > 1,500 \text{ MJ}\cdot\text{ha}^{-1}\cdot\text{mm}\cdot\text{h}^{-1}\cdot\text{day}^{-1}$   
441  $^1\cdot\text{day}^{-1}$  presents a “very high” possibility of fatalities; “very high” number of homeless people;  
442 and “very high” possibility of social, economic and infrastructure damages. In these cases, the  
443 alert system must be activated immediately and the rescue teams must be properly prepared;  
444 (ii)  $1,000 < R_{\text{day}} < 1,500 \text{ MJ}\cdot\text{ha}^{-1}\cdot\text{mm}\cdot\text{h}^{-1}\cdot\text{day}^{-1}$  shows “high” possibility of fatalities, “very  
445 high” possibility for homeless people, and “high” possibility of causing damage to  
446 infrastructure and economy; (iii)  $500 < R_{\text{day}} < 1,000 \text{ MJ}\cdot\text{ha}^{-1}\cdot\text{mm}\cdot\text{h}^{-1}\cdot\text{day}^{-1}$  “medium”  
447 possibility of fatalities in the urban area and “low” possibility in the rural area, “medium”  
448 impact in terms of homelessness, and “medium to low” possibility of causing damage to the  
449 infrastructure and economy; (iv)  $R_{\text{day}} < 500 \text{ MJ}\cdot\text{ha}^{-1}\cdot\text{mm}\cdot\text{h}^{-1}\cdot\text{day}^{-1}$  shows “very low”  
450 possibility of fatalities, “low” number of homeless people, and “low” possibility of economic  
451 and infrastructure losses.

452         According to the classification presented by *Alerta-Rio*, only one event of all the eight  
453 extreme events which caused great human and economic losses, or 14 if the municipalities are  
454 considered separately (Table 3), could be classified as “very high” risk, five as “high”, six as

455 “medium” and two were not classified, meaning they were not considered as causing natural  
456 disasters.

457         Among these events, the 3<sup>rd</sup> largest rainfall accumulated in 24 hours (183.5 mm) was  
458 the cause of the “mega-disaster” observed in MRRJ. According to the *Alerta-Rio*  
459 classification, this event would be classified as “high” risk (not “very high” risk as  $R_{\text{day}}$ ).  
460 Although this event was the 3<sup>rd</sup> largest in terms of precipitation accumulated in 24 hours, it  
461 presented the 2<sup>nd</sup> highest  $R_{\text{day}}$  value ( $2,594 \text{ MJ}\cdot\text{ha}^{-1}\cdot\text{mm}\cdot\text{h}^{-1}\cdot\text{day}^{-1}$ ). This demonstrates how the  
462 proposed index is more comprehensive as a warning of natural disasters.

463         Considering the two events that were not classified by the *Alerta-Rio* since the  
464 accumulated precipitation in 24 hours was below 85 mm, it is observed that these events had  
465  $R_{\text{day}}$  values close to  $1,000 \text{ MJ}\cdot\text{ha}^{-1}\cdot\text{mm}\cdot\text{h}^{-1}\cdot\text{day}^{-1}$ , which caused 71 fatalities. The other event,  
466 although no fatality was observed, affected more than 100 thousand inhabitants and left 144  
467 families homeless. The alert system would have been triggered when applying  $R_{\text{day}}$ , and much  
468 of the impact would have been minimized.

469         Among the three criteria studied by Oliveira et al. (2016), criterion A is the least  
470 restrictive. Of the events presented in Table 3, only one (occurred on Jan-12, 2011) in the  
471 municipality of Petrópolis is not considered to cause landslides, when the precipitation  
472 accumulated in 72 hours is analyzed. The same result is obtained for criterion B.

473         Criterion C constraints the occurrence of landslides. The event that hit Petrópolis in  
474 12/01/2011 was discarded as a cause of landslides in criteria A and B, as well as the event of  
475 Jan-15, 2016) in Teresópolis. These two events are the same that are not classified by *Alerta-*  
476 *Rio*, and together they affected thousands of people. Oliveira et al. (2016) emphasize that  
477 thresholds established for the most restrictive criteria do not separate events with landslides  
478 from those without landslides but are identified together with multiple disasters.



479 Comparing both early warning indexes (Figure 5) spatially, one can observe a  
480 sensitivity of the Rday index, especially in the rainfall hazards in which fatalities were  
481 observed. Examples are the events of 2001, 2006, 2007, 2011, and 2016. The *Alerta-*  
482 *Rio* index would emit a “high” warning in all these years, while Rday displays an “every  
483 high” warning for fatalities. Call attention 2011 event, the most severe rainfall hazard in  
484 Brazil. In this case, only a tiny spot would be warned as a “very high” warning, being the  
485 most significant part of the most affected area receiving a “high” warning. Otherwise, Rday  
486 would emit a “very high” possibility for fatalities in most of this area. We can see that more  
487 than 400 people died because of this event. In this direction, the event of 2016 would be  
488 understood as a “mean” warning using *Alerta-Rio*, whereas Rday would emit a “very high”  
489 warning (34 fatalities + more than 150,000 people displaced). Therefore, proposing Rday as a  
490 new early warning index proved to be more sensitive and more accurate with the impacts  
491 provoked by the rainfall because this index encompasses more information regarding the  
492 nature of heavy rainfall. Besides, it is easy to calculate and apply as a warning index for the  
493 MRRJ.

494 It should be noted that the occurrence of natural disasters in a region is inevitable since  
495 they depend on climatic variables. However, the consequences caused by these events not  
496 only depend on climatic factors, but also on political, social, and economic factors. Thus, an  
497 effective EWS must comprise four main components: knowledge of risk, monitoring,  
498 communication structures and efficient alerts, and lastly precautions, all of which need  
499 application of efficient public policies.

500

## 501 **5. CONCLUSIONS**

502  $R_{day}$  addresses fundamental physical aspects associated with precipitation, its energy,  
503 as well as the mean and maximum intensities over a 30-minute time interval, being more

504 sensitive than those which have been used in Brazil. Considering warning indices based only  
505 on the total rainfall or intensity of rainfall has not been shown to be sufficient to understand  
506 the complex dynamics of an extreme rainfall event, as its consequences are not only caused  
507 by water accumulation, but mainly by the dissipation of accumulated energy.  $R_{\text{day}}$  values can  
508 integrate national databases on the most vulnerable areas and specify risk management  
509 strategies and disaster response approaches, especially in places with the highest  
510 concentrations of exposed people. Further conclusions are:

- 511 a) The  $R_{\text{day}}$  model had superior performance of other studies with the same model  
512 and can be applied to additional studies related to rainfall disasters in Brazil.
- 513 b) All events with  $R_{\text{day}} > 1,500 \text{ MJ}\cdot\text{ha}^{-1}\cdot\text{mm}\cdot\text{h}^{-1}\cdot\text{day}^{-1}$  would fatally impact the region,  
514 and therefore areas historically affected by these events should be considered more  
515 prone to natural disasters.
- 516 c) Using the fitted model for  $R_{\text{day}}$  estimates, it was found that the municipality of  
517 Nova Friburgo, and the south of the municipality of Petrópolis are very vulnerable  
518 to natural disasters from the climatic point of view, with the highest  $R_{\text{maxday}}$   
519 values.
- 520 d) January was historically the period with the highest daily erosivity values, in  
521 which all precipitation events used for developing the  $R_{\text{maxday}}$  map occurred in the  
522 first or second half of this month.

523

## 524 **ACKNOWLEDGMENTS**

525 We acknowledge the Improvement of Higher Educational Personnel – CAPES [grant  
526 number 88882.306661/2018-01]; the National Council for Scientific and Technological  
527 Development – CNPQ [grant number 301556/2017-2]; and FAPEMIG [grant number PPMX-  
528 545/18] for supporting and funding this work.

529 **References**

530 Angulo-Martínez, M., Beguería, S. (2009). Estimating rainfall erosivity from daily  
531 precipitation records: a comparison among methods using data from the Ebro Basin (NE  
532 Spain). *Journal of Hydrology* 379 (1-2), 111-121.

533

534 Brasil. Ministério de Minas e Energia (2012). Seleção dos Municípios Críticos a  
535 Deslizamentos: Nota Explicativa. CPRM, Rio de Janeiro.

536

537 Brito, T.T., Oliveira Jr., J.F., Lyra, G.B., Gois, G., Zeri, M. (2016). Multivariate analysis  
538 applied to monthly rainfall over Rio de Janeiro state, Brazil. *Meteorology and Atmospheric  
539 Physics* 129, 469-478.

540

541 Brooks, H.E., Stensrud, D.J., 2000. Climatology of heavy rain events in the United States  
542 from hourly precipitation observations. *Mont. Weather Rev.* 4, 1194-1201.  
543 [https://doi.org/10.1175/1520-0493\(2000\)12860;1194:cohrei62;2.0.co;2](https://doi.org/10.1175/1520-0493(2000)12860;1194:cohrei62;2.0.co;2).

544 Busch, A., Amorim, S.N.D. (2011). A Tragédia da Região Serrana do Rio de Janeiro em  
545 2011: Procurando respostas. ENAP, Brasília.

546

547 Calvello, M., D’Orsi, R.N., Piciullo L., Paes, N., Magalhães, M., Lacerda, W.A. (2015). The  
548 Rio de Janeiro early warning system for rainfall-induced landslides: Analysis of performance  
549 for the years 2010–2013. *Internatinal Journal Disaster Risk Reduction Reduct.* 12, 3-15.  
550 <https://doi.org/10.1016/j.ijdrr.2014.10.005>.

551

- 552 Cardozo, C.P., Lopes, E.S., Monteiro, A.M.V. (2018). Shallow landslide susceptibility  
553 assessment using SINMAP in Nova Friburgo (Rio de Janeiro, Brazil). *Revista Brasileira de*  
554 *Cartografia* 4, 1206-1230. <https://doi.org/10.14393/rbcv70n4-46139>.  
555
- 556 Cardozo, C.P., Monteiro, A.M.V. (2019). Assessing social vulnerability to natural hazards in  
557 Nova Friburgo, Rio de Janeiro mountain region, Brazil. *REDER* 2, 71-83.  
558
- 559 CEPED. (2013). *Atlas Brasileiro de Desastres Naturais: 1991-2010*, second ed. Ceped, Santa  
560 Catarina.  
561
- 562 Coelho Netto, A.L., Sato, A.M., Avelar, A.S., Vianna, L.G.G., Araújo, I.S., Ferreira, D. L.A.,  
563 Lima, P.H., Silva, A.P.A., Silva, R.P. (2013). January 2011: The extreme landslide disaster in  
564 Brazil. In: Margottini, C., Canuti, P., Sassa, K. (Eds.), *Landslide Science and Practice*.  
565 Heidelberg, Springer, pp. 377-384.  
566
- 567 Dolif, G., Nobre, C. (2012). Improving extreme precipitation forecasts in Rio de Janeiro,  
568 Brazil: Are synoptic patterns efficient for distinguishing ordinary from heavy rainfall  
569 episodes? *Atmos. Sci. Lett.* 3, 216-222. <https://doi.org/10.1002/asl.385>.  
570
- 571 Fernandes, L.G., Rodrigues, R.R. (2018). Changes in the patterns of extreme rainfall events in  
572 southern Brazil. *International Journal of Climatology* 38, 1337-1352.  
573 <https://doi.org/10.1002/joc.5248>.  
574
- 575 Freitas, C.M., Carvalho, M.L., Ximenes, E.F., Arraes, E.F., Orlando, J. (2012).  
576 Vulnerabilidade socioambiental, redução de riscos de desastres e construção da resiliência:

- 577 Lições do terremoto no Haiti e das chuvas fortes na Região Serrana, Brasil. *Ciência e Saúde*  
578 *Coletiva* 17, 1577-1586. <https://doi.org/10.1590/S1413-81232012000600021>.  
579
- 580 Groisman, P.Y., Knight, R.W., Karl, T.R. (2001). Heavy precipitation and high streamflow in  
581 the contiguous United States: Trends in the twentieth century. *Bull. Amer. Meteor. Soc.* **82**,  
582 219–246. [https://doi.org/10.1175/1520-0477\(2001\)082<0219:HPAHSI>2.3.CO;2](https://doi.org/10.1175/1520-0477(2001)082<0219:HPAHSI>2.3.CO;2).  
583
- 584 Groisman, P.Y., Knight, R.W., Karl, T.R. (2012). Changes in intense precipitation over the  
585 central United States. *J. Hydrometeorol.* 1, 47-66. <https://doi.org/10.1175/JHM-D-11-039.1>.  
586
- 587 Guzzetti, F., Peruccacci, S., Rossi, M., Stark, C.P. (2007). Rainfall thresholds for the initiation  
588 of landslides in central and southern Europe. *Meteorology and Atmospheric Physics* 98, 239-  
589 267. <https://doi.org/10.1007/s00703-007-0262-7>.  
590
- 591 IBGE (2010). Census. [http://www.ibge.gov.br/home/estatistica/populacao/censo2010/](http://www.ibge.gov.br/home/estatistica/populacao/censo2010/default.shtm)  
592 [default.shtm](http://www.ibge.gov.br/home/estatistica/populacao/censo2010/default.shtm) (accessed on January 17, 2020).  
593
- 594 De Maria, I.C. (1994). Cálculo da erosividade da chuva, in: Instituto Agronômico de  
595 Campinas. Manual de programas de processamento de dados de campo e de laboratório para  
596 fins de experimentação em conservação do solo. IAC-SCS.  
597
- 598 McGregor, K.C., Mutchler, C.K. (1976). Status of the R-factor in northern Mississippi. In:  
599 Toy, T.J., Foster, G.R., Renard, K.G. *Soil Erosion: Prediction and control*. Soil Conservation  
600 Society America, pp. 135-142.  
601

- 602 Mello, C.R., Alves, G.J., Beskow, S., Norton, L.D. (2020). Daily rainfall erosivity as an  
603 indicator for natural disasters: assessment in mountainous regions of southeastern Brazil.  
604 *Natural Hazards* 103, 947-966. <https://doi.org/10.1007/s11069-020-04020-w>.
- 605
- 606 Mello, C.R., Ávila, L.F., Viola, M.R., Curi, N., Norton, L.D. (2015). Assessing the climate  
607 change impacts on the rainfall erosivity throughout the twenty-first century in the Grande  
608 River Basin (GRB) headwaters, southeastern Brazil. *Environmental Earth Science* 73, 8683-  
609 8698. <https://doi.org/10.1007/s12665-015-4033-3>.
- 610
- 611 Mendes, R.M., Andrade, M.R.M., Tomasella, J., Moraes, M.A.E., Scofield, G.B. (2018).  
612 Understanding shallow landslides in Campos do Jordão municipality – Brazil: Disentangling  
613 the anthropic effects from natural causes in the disaster of 2000. *Natural Hazard Earth Science*  
614 *System* 18, 15-30. <https://doi.org/10.5194/nhess-18-15-2018>.
- 615
- 616 Nash, J.E. & Sutcliffe, J.V. (1970). River flow forecasting through conceptual models part I: a  
617 discussion of principles. *Journal of Hydrology* 10, 282-290.
- 618
- 619 Oliveira, N.S., Rotunno Filho, O.C., Maton, E., Silva, C. (2016). Correlation between rainfall  
620 and landslides in Nova Friburgo, Rio de Janeiro—Brazil: A case study. *Environmental Earth*  
621 *Science* 75, number 1358. <https://doi.org/10.1007/s12665-016-6171-7>.
- 622
- 623 [Pinto](#), L.C., Mello, C.R., Norton, L.D., Poggere, G.C., Owens, P.R., [Curi](#), N. (2018). A  
624 hydrogeological approach to a mountainous Clayey Humic Dystrudept in the Mantiqueira  
625 range, southeastern Brazil. *Scientia Agricola* 75, 60-69. [http://dx.doi.org/10.1590/1678-992x-](http://dx.doi.org/10.1590/1678-992x-2016-0144)  
626 [2016-0144](http://dx.doi.org/10.1590/1678-992x-2016-0144).

- 627 Pristo, M.V.J., Dereczynski, C.P., Souza, P.R., Menezes, W.F. (2018). Climatologia de  
628 chuvas intensas no município do Rio de Janeiro. Rev. Bras. Meteorol. 4, 615-630.  
629
- 630 Reboita, M.S., Gan, M.A., Rocha, R.P., Ambrizzi, T. (2010). Regimes de precipitação na  
631 América do Sul: Uma revisão bibliográfica. Revista Brasileira de Meteorologia 2, 185-204.  
632 <http://dx.doi.org/10.1590/S0102-77862010000200004>.  
633
- 634 Richardson, C.W., Foster, G.R., Wright, D.A. (1983). Estimation of erosion index from daily  
635 rainfall amount. Transactions of the ASABE 26, 153-156.  
636 <https://doi.org/10.13031/2013.33893>.  
637
- 638 Wang, Y., Tan, S., Liu, B., Yang, Y. (2017). Estimating rainfall erosivity by incorporating  
639 seasonal variations in parameters into the Richardson model. Journal of Geographical Science  
640 27, 275-296. <https://doi.org/10.1007/s11442-017-1376-6>.  
641
- 642 Wischmeier, W.H., Smith, D.D. (1958). Rainfall energy and its relationship to soil loss.  
643 Transactions of the American Geophysical Union 39, 285-291.  
644 <https://doi.org/10.1029/TR039i002p00285>.  
645
- 646 Wischmeier, W.H., Smith, D.D. (1978). Predicting rainfall erosion losses: A guide to  
647 conservation planning. USDA, Washington.  
648
- 649 Xie, Y., Liu, B., Nearing, M.A. (2002). Practical thresholds for separating erosive and non-  
650 erosive storms. Transactions of the ASAE 45, 1843-1847.  
651 <https://doi.org/10.13031/2013.11435>.

- 652 Xie, Y., Yin, S., Liu, B., Nearing, M., Zhao, Y. (2016). Models for estimating daily rainfall  
653 erosivity in China. *Journal of Hydrology* 535, 547-558.  
654 <https://doi.org/10.1016/j.jhydrol.2016.02.020>.
- 655
- 656 Xu, L., Meng, X., Xu, X. (2014). Natural hazard chain research in China: A review. *Natural*  
657 *Hazards* 70, 1631-1659. <https://doi.org/10.1007/s11069-013-0881-x>.
- 658
- 659 Yang, X., Yu, B. (2015). Modelling and mapping rainfall erosivity in New South Wales,  
660 Australia. *Soil Research* 53, 178-189. <https://doi.org/10.1071/SR14188>.
- 661
- 662 Yin, S., Xie, Y., Nearing, M.A., Wang, C. (2007). Estimation of rainfall erosivity using 5-to  
663 60-minute fixed-interval rainfall data from China. *Catena* 70, 306-312.  
664 <https://doi.org/10.1016/j.catena.2006.10.011>.
- 665
- 666 Yu, B., Rosewell, C.J. (1996). Rainfall erosivity estimation using daily rainfall amounts for  
667 South Australia. *Australian Journal of Soil Research* 53, 721-733.  
668 <https://doi.org/10.1071/SR9960721>.



**ARTICLE 2 - RAINFALL DISASTERS UNDER THE CHANGING CLIMATE: A  
CASE STUDY FOR THE RIO DE JANEIRO MOUNTAINOUS REGION**

Article published in the journal *Natural Hazards*, ISSN: 0921-030X, being published according to the publication rules.

**Rainfall disasters under the changing climate: a case study for the Rio de Janeiro  
mountainous region**

# Rainfall disasters under the changing climate: a case study for the Rio de Janeiro mountainous region

## Abstract

Climate change impacts the erosive power of rain, influencing mountainous landscapes' vulnerability to natural disasters. This study evaluated the spatiotemporal projections of daily rainfall erosivity ( $R_{\text{day}}$ ), an efficient warning index for rainfall disasters, under climate change. The objectives of this study were to project spatially  $R_{\text{day}}$  across the Mountain Region of the Rio de Janeiro State (MRRJ), one of the most vulnerable regions to rainfall disasters in Brazil, and to analyze the frequencies of  $R_{\text{day}}$  values throughout the 21<sup>st</sup> century. Two greenhouse gas emission scenarios (RCP 4.5 and 8.5), approximating the current status in South America, and a high-resolution climate model (the HadGEM2-ES physically downscaled to 5 km resolution by the Eta/CPTEC model) were applied to estimate daily rainfall values over the MRRJ. The mapping of the maximum  $R_{\text{day}}$  values in 30 years ( $R_{\text{maxday}}$ ) showed that the entire MRRJ is highly susceptible to rainfall disasters throughout the 21<sup>st</sup> century, with intensification around 2040-2071. Urban areas, where fatalities have been recorded, have been the most vulnerable due to the high frequency of heavy rainfall. The projections for the 21<sup>st</sup> century indicated that 17 (under RCP4.5) and 15 (under RCP8.5) events like the "mega-disaster" could hit the study region. Thus, public policy efforts should focus on effective stormwater management actions to mitigate the impacts caused by such disastrous events in this century.

**Keywords:** daily rainfall erosivity; natural disasters; mountainous region; climate change Brazil.

## Introduction

Natural disasters are the consequences of extreme events that cause significant impacts on the social, economic, environmental, or even psychological balance of people (Alexander et al., 2021). For example, floods and landslides caused by heavy rainfall are the most frequent natural disasters that affect humanity, causing thousands of deaths annually worldwide (Alexander et al., 2021).

Based on several studies worldwide, Lukic et al. (2013) reported that natural hazards have increased over time. From an economic point of view, the damages caused by natural hazards increased from several tens of billion dollars in the first seven decades of the last century to 380 billion dollars in 2011. The same was observed for fatalities, which globally impacted more than 24,000 lives per year between 1977 and 1997 to over 70,000 in 2011. Analyzing statistics published by Lukic et al. (2013), in America continent, 63% of the hazards are due to hydrological and meteorological events, such as severe storms, floods, and landslides. In Asia and Africa, 80% and 36% of natural hazards have occurred because of hydrological and meteorological events. In Europe and Oceania, natural hazards are considerably lower, 12% and 8%, from hydrological and meteorological causes.

Significant impacts of climate change have been observed in extreme heat, droughts, coastal flooding, erosion, wildfires, floods, and landslides. In South America, these drivers impact agricultural production, water availability, desertification of tropical biomes, and mass change in glaciers, which increase floods, soil erosion, and landslides (IPCC, 2022).

Natural disasters have hit South America, increasing the trends in climatic variability and extreme events, such as rainfall and droughts. In some regions of South America, especially in the southeast, a trend in precipitation has been observed. Projects from RCP4.5 and RCP8.4 scenarios indicate an increase of 25% in this

41 region of South America (IPCC, 2022), which can potentially increase the occurrence of rainfall hazards in  
42 several regions, like the mountains of southeast Brazil, where Rio de Janeiro is located. It is essential to highlight  
43 the magnitude and frequency of extreme rainfall in South America and its projections. Chou et al. (2014a)  
44 projected a decrease in heavy rainfall considering an increase of 1.5°C; however, Imbach et al. (2018) projected  
45 an increase in the frequency of the R50mm, i.e., an increase in the number of days with rainfall greater than 50  
46 mm for global warming of 2°C and 4°C.

47 In Brazil, landslides and floods are the main ones responsible for the greatest impacts from natural  
48 hazards with a number of fatalities (CEPED, 2012). These hazards are triggered by extreme rainfall, leading to  
49 many fatalities in this country every year, especially in areas geomorphological prone to landslides, such as the  
50 mountains region of southeast Brazil. Thus, the increase in the frequency and intensity of extreme rainfall, in  
51 combination with the high degree of susceptibility of the population in risk areas, has triggered these disasters in  
52 the country, especially in mountainous regions with high geological risk (Fernandes and Rodrigues, 2018;  
53 Amorim and Chaffe, 2019). Some mountainous regions of Brazil are places where geomorphological features,  
54 deforestation of the Atlantic Forest, recurrent heavy rainfall (Freitas et al. 2012), and the uncontrolled growth of  
55 urban areas potentiate the consequences arising from natural disasters (Mello et al. 2020). One of the regions  
56 most affected by extreme rainfalls is the Mountain Region of the Rio de Janeiro State (MRRJ), which is one of  
57 the most vulnerable to rainfall disasters in the country (Freitas et al., 2012; Brasil, 2012; Bitar, 2014; Oliveira et  
58 al. 2016). This region suffered many events that resulted in several fatalities, such as the so-called "mega-  
59 disaster" in 2011 (Alves et al. 2022). The most recent hit the city of Petropolis in February 2022, causing the  
60 death of 231 people (Alcântara et al., 2022). This event, in meteorological terms, was extraordinary, bringing  
61 252 mm of rain in three hours.

62 Determining indexes applied to alert/warning systems to mitigate the impacts caused by rainfall  
63 disasters is always challenging. The document of the World Conference for Disaster Reduction in Japan in 2005  
64 warns of the need to develop indicator systems at different levels of scope to enable a better diagnosis and  
65 response to risk situations and vulnerability by decision-makers (Silva et al. 2016). In this sense, some studies  
66 have evaluated the efficiency of the Monitoring and Alert System (MAS) ("Early Warning System") indicators  
67 in reducing risks related to economic impacts, in addition to the risks of fatalities (Webster, 2013; Alvalá et al.  
68 2019). As intense rainfalls trigger these events in Brazil, indexes are used as an early warning based on their  
69 temporal behavior. Weather forecasting can be reliable if made up to 72 hours in advance (Oliveira et al. 2016).  
70 Thus, rainfall (accumulated and its intensity) composes most of the MASs (Calvello et al., 2015; Mello et al.,  
71 2020; Alves et al., 2022).

72 Some indexes are widely used in Brazil and the world, such as the accumulated rainfall in the last 24,  
73 48, 72, and 96 hours, the rainfall intensity (mm/h), or their combinations (Oliveira et al. 2016; Calvello et al.  
74 2015; Silva et al. 2020). Some studies also used rainfall erosivity and other rainfall indexes to identify areas  
75 more prone to landslides in Europe. Lukic et al. (2021) applied the Angot Precipitation Index to study rainfall  
76 erosivity behavior in the Vojvodina region, Serbia and observed a good performance of this index to identify the  
77 aggressiveness of rainfall and its correlation with soil water erosion. Ponjiger et al. (2021) applied the daily  
78 rainfall erosivity and respective density erosivity to identify areas more susceptible to water erosion in the  
79 Pannonian Basin, Central Europe. Although they applied the model and respective parameters proposed by  
80 Zhang et al. (2002) to China, they identified the seasons in which rainfall erosivity has been marked, enhancing

81 the assessment of the aggressiveness of rainfall erosivity in southern Europe. Morar et al. (2021) also studied  
82 rainfall erosivity as a predictor for natural hazards in the Ciuperca region, Romania, using monthly rainfall data.  
83 Besides rainfall erosivity, they applied the Precipitation Concentration Index (PCI) and Modified Fournier Index  
84 (MFI), both good indexes related to the aggressiveness of rainfall. In another study carried out in Belgrade,  
85 Serbia, Lukic et al. (2018) also applied the PCI and MFI and observed a moderate aggressiveness of rainfall,  
86 which, together with the geological features, demonstrated the vulnerability of the studied region to natural  
87 hazards triggered by rainfall.

88 However, these indexes may be inefficient in some cases (Calvello et al., 2015; Mello et al., 2020).  
89 Thus, Mello et al. (2020) established an alert climate index ( $R_{\text{day}}$ ) related to the maximum daily rainfall erosivity  
90 for the Mantiqueira range region (Southeast Brazil) based on the impact of the rain, rainfall amount, and rainfall  
91 intensity. This index is based on rainfall erosivity, a climatic index that portrays the impacts of energy dissipated  
92 by raindrops on the surface. Thus, it is a more comprehensive index than the others to predict hazards, especially  
93 fatalities. This concept was initially proposed and defined by Wischmeier and Smith (1958) as the product  
94 between the kinetic energy of raindrops ( $E_k$ ) and the maximum rainfall intensity in 30 consecutive minutes ( $I_{30}$ ),  
95 designated as  $EI_{30}$ . When applied on a daily scale, it can help better understand the role of heavy rainfall in  
96 natural disasters (Alves et al., 2022; Mello et al., 2020).

97 A rainfall network with a temporal resolution  $< 15$  min for the computation of daily rainfall erosivity  
98 ( $R_{\text{day}}$ ) is often lacking in Brazil. Thus, applying a model for  $R_{\text{day}}$  estimation based on daily rainfall data, which  
99 are more accessible and spatially distributed, is critical to linking heavy rainfall events to natural disasters (Chen  
100 et al., 2020). In this aspect, Alves et al. (2022) developed a similar index for MRRJ. This index is based on Yu  
101 and Rosewell's (1996) study, which proposed a method to estimate the seasonality of  $R_{\text{day}}$ , and on the index  
102 established by Mello et al. (2020).

103 In this context, climate change and its impacts on the magnitude and frequency of rainfall disasters are  
104 uncertain, especially in regions with significant orographic influences (Lyra et al., 2017). Disasters involving  
105 landslides have become more frequent and severe during the last decades (CEPED, 2013), especially in  
106 mountainous regions of Brazil (Mello et al., 2020). Such facts demonstrate evident changes in the heavy rainfall  
107 pattern (IPCC, 2013), and rapid population growth, which result in disorganized urbanization (IPCC, 2022).

108 It is a fact that climate change has impacted the rainfall pattern in Brazil, with clear changes in rainfall  
109 erosivity. However, most studies have focused on annual rainfall erosivity (or RUSLE's R-factor) (Riquetti et al.,  
110 2020; Mello et al., 2015), which needs to be further understood as impacts on extreme rainfall events. This study  
111 brings as novelty an assessment of climate change impacts on daily rainfall erosivity ( $R_{\text{day}}$ ), being the first  
112 investigation in this regard in Brazil. Studies of climate change impacts on daily rainfall remain little studied in  
113 tropical and mountainous regions, and their contribution to preventing rainfall hazards is essential. Using a daily  
114 rainfall erosivity model, it is possible to assess the frequency of heavy rainfall, respective  $R_{\text{day}}$ , and impacts of  
115 rainfall disasters using daily rainfall projections over the century.

116 The objectives of this study were to i) apply a seasonal model to calculate  $R_{\text{day}}$  for the MRRJ throughout  
117 the 21<sup>st</sup> century, using a high-resolution climate model (HadGEM2-ES physically regionalized by the ETA-  
118 CPTEC model in the 5 km spatial scale – the 5-km Eta-HadGEM2-ES), and the RCP4.5 and 8.5 IPCC scenarios,  
119 ii) map the maximum daily rainfall erosivity ( $R_{\text{maxday}}$ ) to assess the most vulnerable areas of MRRJ throughout

120 the present century, and iii) to project the frequency of  $R_{\text{day}} > 500 \text{ MJ mm (ha h)}^{-1} \text{ day}^{-1}$  (a threshold for the  
 121 harmost events) throughout the 21<sup>st</sup> century.

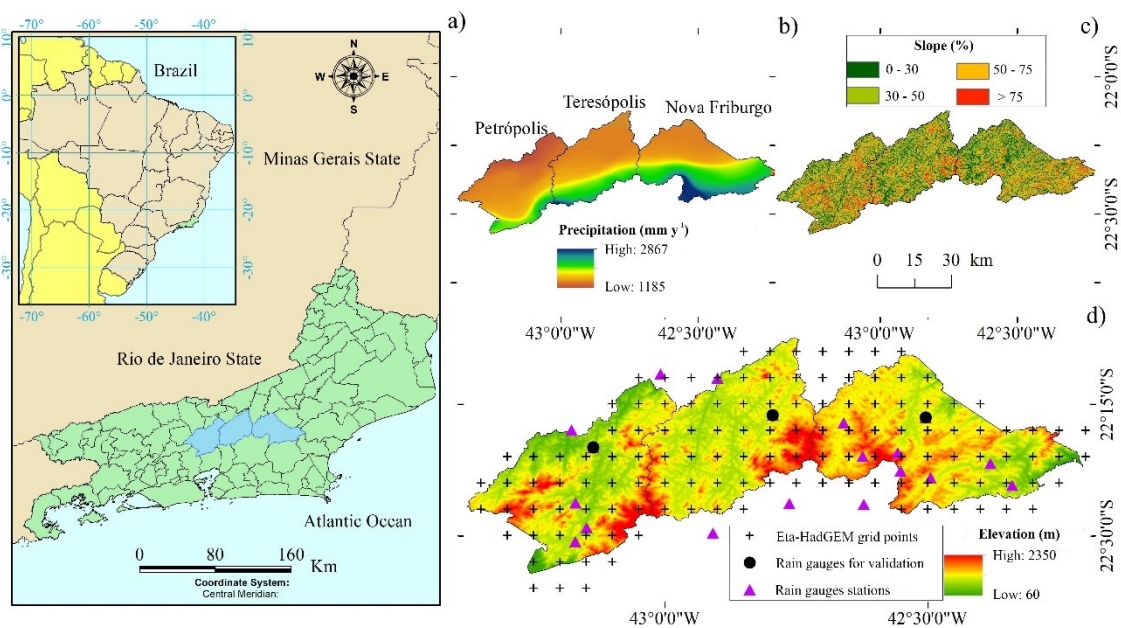
122

## 123 Material and Methods

### 124 *Some aspects of the mountain region of the Rio de Janeiro State (MRRJ)*

125 The MRRJ is located in the Serra do Mar and is characterized by mountainous to steep relief, with  
 126 altitudes ranging from 400 to 2350 meters (Figure 1). It is located in the unit called "Planalto Reverso" (Garcia  
 127 and Francisco, 2013), and the soils are predominantly shallow, moderately permeable, and have low natural  
 128 fertility (Pinto et al., 2018).

129 The geographic location of the three most populous municipalities, Petrópolis (792 km<sup>2</sup>), Teresópolis  
 130 (773 km<sup>2</sup>), and Nova Friburgo (936 km<sup>2</sup>), and the digital elevation model for the entire region are shown in  
 131 Figure 1. The location of the rainfall stations from the National Water and Sanitation Agency (ANA) and the 130  
 132 grid points for which the daily rainfall data of the climate projections used in this study are also presented. These  
 133 three municipalities represent almost 80% of the entire MRRJ population (IBGE, 2010) and have been the most  
 134 affected by rainfall disasters in Brazil (Alves et al., 2022; Coelho Netto et al., 2013).



135

136 **Figure 1.** The geographical location of MRRJ (a), with emphasis on Nova Friburgo, Petrópolis, and Teresópolis,  
 137 annual precipitation map (b), relief (slope) map (c), and the grid points obtained by the 5-km Eta-HadGEM2-ES  
 138 model and locations of the ANA rain-gauges (d).

139

140 The entire MRRJ was originally covered by Atlantic Forest, which was removed to make way for  
 141 plantations, pastures, and urban centers. Despite currently being fragmented and degraded, especially around  
 142 urban areas, the Atlantic Forest still represents more than 50% of the region's vegetation cover (Coelho Netto et  
 143 al., 2013; Garcia and Francisco, 2013; Cardozo and Monteiro, 2019). Garcia and Francisco (2013) found that this  
 144 biome is present in the steepest and most elevated places. It suffers from fires during the dry period, resulting in  
 145 the destruction of its vegetation cover, making the surface more susceptible to landslides caused by rain in the  
 146 summer.

The climate of the MRRJ is Cwb (Köppen climate-type), meaning a mild temperate climate with dry winters and rainy summers. The average annual temperature is approximately 16°C and the average temperature of the hottest month is below 22°C (Coelho Netto et al. 2013). Summers are rainy (more than 70% of rainfall occurs between October and March) (André et al. 2008), and winters are cold and dry (Dourado et al. 2012). The rainfall pattern in the MRRJ is driven by several climatic phenomena, such as i) frontal systems, which act throughout the year and which, combined with the humidity of the Atlantic Ocean, bring significant amounts of rain, ii) convective rains in summer, iii) South Atlantic Convergence Zone (SACZ) during the summer, iv) orographic effects, v) tropical and subtropical cyclones, and vi) maritimity (Reboita et al. 2010).

#### **Daily rainfall erosivity ( $R_{day}$ ) model to MRRJ**

The seasonal model of daily rainfall erosivity fitted by Alves et al. (2022) is based on the studies by Yu and Rosewell (1996) and was used for this study.

$$R_{day} = 3.3888 \cdot \left[ 1 + 0.4659 \cdot \cos\left(\frac{2 \cdot \pi \cdot j}{24} - \frac{\pi}{6}\right) \right] \cdot P_{day}^{1.2028} \quad (1)$$

In which  $j$  is the fortnight (ranging from 1 to 24) and  $P$  is the daily precipitation in a 24-hour interval (mm). It is important to highlight that this model represents the MRRJ since it was determined based on data from 68 stations with precipitation data with a temporal resolution of 10 minutes. The precision statistics presented and discussed by the author showed satisfactory results for estimating the  $R_{day}$  (calibration:  $C_{NS} = 0.51$ ;  $P_{bias} = -0.56$ ) and (validation:  $C_{NS} = 0.50$ ;  $P_{bias} = -2.22$ ).

Equation 1 was applied to the daily rainfall data obtained from the ANA rain-gauges to the historical data (baseline) and the climate projections provided by the Global Circulation Climate Model (GCM) (HadGEM2-ES) downscaled by a physical model, the Eta/CPTEC (5-km Eta-HadGEM2-ES).

Maximum daily rainfall erosivity ( $R_{maxday}$ ) maps were developed considering the highest  $R_{day}$  values observed at each grid point provided by the 5-km Eta-HadGEM2-ES model (Figure 1) for the historical period (1961-2005) and three different periods throughout the 21st century (2006-2040, 2041-2070 and 2071-2099). In addition, percentage variation maps of future periods were prepared and referred to the historical data. These maps make it possible to detect areas with greater susceptibility to natural disasters caused by extreme precipitation events throughout the century.

#### **Climate change projections of $R_{day}$ using a high-resolution climate model for the MRRJ**

The Eta Regional Climate Model (RCM) was refined by Chou et al. (2012) and Marengo et al. (2012) to provide downscaling of climate change projections in South America at a spatial resolution of  $0.20^\circ \times 0.20^\circ$  (20 km horizontally and 38 layers vertically) nested to the HadGEM2-ES, MIROC5, BESM and CANESM2 global climate models (GCMs). Its most recent version was described in detail by Mesinger et al. (2012) and evaluated for long-term simulations by Pesquero et al. (2010), Flato et al. (2013), and Chou et al. (2012, 2014a, b).

The orographic influence on precipitation should be considered to improve the simulation results (Brito et al., 2016; André et al., 2008). Therefore, the spatial resolution of 20 km produces insufficient results for analyzing the frequency of extreme events that cause natural rainfall disasters (Chou et al., 2014a). Thus, a downscaling process was carried out using the Eta-CPTEC model for a 5-km resolution to overcome the coarse

187 resolution (20 km), nesting it to the HadGEM2-ES GCM under the RCP4.5 and RCP8.5 emission scenarios in  
 188 the period from 1961 to 2100. However, due to the high computational demand, only the Eta-HadGEM2-ES was  
 189 regionalized for the 5 km scale and is only available for Southeastern Brazil (where MRRJ is located). Lyra et al.  
 190 (2017) detailed this higher spatial resolution version.

191 In the Fifth Assessment Report (AR5) of the Intergovernmental Panel on Climate Change (IPCC, 2013),  
 192 greenhouse gas concentration scenarios are based on two "Representative Concentration Pathways" (RCP),  
 193 which are expressed in terms of radiative forcing to the end of the 21st century. The scenarios used in this study  
 194 were RCP8.5 and RCP4.5 (Van Vuuren et al. 2011), the only ones available for South America. RCP4.5 is  
 195 considered an intermediate scenario that assumes greenhouse gas emissions stabilization from the middle of the  
 196 21st century. This scenario considers a global radiative forcing of approximately  $4.5 \text{ W.m}^{-2}$ . On the other hand,  
 197 RCP8.5 is a scenario that considers an increase in greenhouse gas emissions by the end of the century, meaning  
 198 that no implementation of climate policies and continued acceleration of the use of fossil fuels.

199 Historical (baseline) data (1961-2005) and climate projections (2006-2099) of daily rainfall for  
 200 calculating  $R_{\text{day}}$  values considering both scenarios were obtained from the Weather Forecast and Studies Center  
 201 of the National Institute for Space Research (CPTEC/INPE) on the platform called "PROJETA" (Holbig et al.  
 202 2018) (<https://projeta.cptec.inpe.br/#/about>).

203 The validation of the 5-km Eta-HadGEM2-ES model to estimate  $R_{\text{day}}$  was conducted with the  
 204 application of the seasonal model of daily erosivity in the period from 1980 to 2005 (26 years) to calculate the  
 205 long-term annual average rainfall erosivity (R-factor) considering the data obtained from three ANA rain-gauge  
 206 stations and the 5-km Eta-HadGEM2-ES for the same period. Daily rainfall  $< 13 \text{ mm}$  was not considered  
 207 erosive, according to the Alves et al. (2022) study, and thus was not considered in the R-factor calculation.

### 209 ***Critical thresholds of $R_{\text{day}}$ MRRJ***

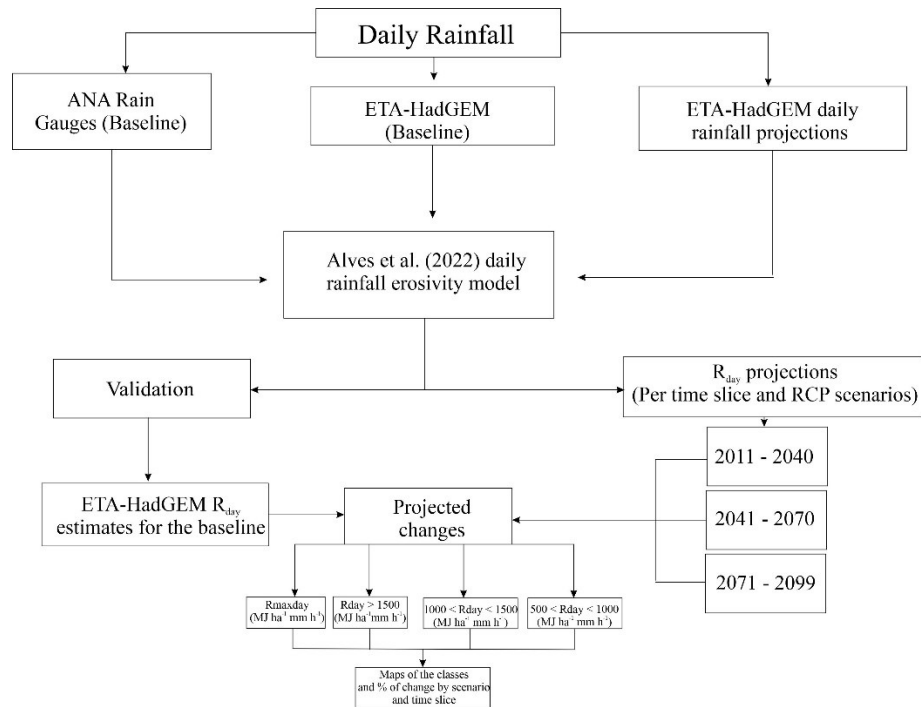
210  $R_{\text{day}}$  thresholds are values proposed to identify and alert areas most vulnerable to natural disasters  
 211 (Mello et al. 2020). These limits have been established through a joint analysis of  $R_{\text{day}}$  values calculated for  
 212 rainfall events that caused disasters concomitantly with the consequences observed in recent decades. As a result,  
 213 the following values were proposed for the MRRJ by Alves et al. (2022):

- 214 i)  $R_{\text{day}} > 1,500 \text{ MJ.ha}^{-1}.\text{mm.h}^{-1}.\text{day}^{-1}$ : "very high" possibility of fatalities; "very high" number of  
 215 homeless; and "very high" possibility of damage in general
- 216 ii) ii)  $R_{\text{day}}$  between 1,000 and 1,500  $\text{MJ.ha}^{-1}.\text{mm.h}^{-1}.\text{day}^{-1}$ : presents a "high" possibility of  
 217 fatalities, a "very high" number of homeless, and a "high" possibility of causing damage to  
 218 infrastructure and economy
- 219 iii) iii)  $R_{\text{day}}$  between 500 and 1,000  $\text{MJ.ha}^{-1}.\text{mm.h}^{-1}.\text{day}^{-1}$ : "medium" possibility of fatalities in  
 220 urban areas and "low" in rural areas, "medium" impact in terms of homeless, and "medium"  
 221 possibility of causing damage to infrastructure and economy
- 222 iv) iv)  $R_{\text{day}} < 500 \text{ MJ.ha}^{-1}.\text{mm.h}^{-1}.\text{day}^{-1}$ : "very low" possibility of fatalities, a "low" number of  
 223 homeless, and a "low" possibility of damage to the economy and infrastructure.

224  
 225 The established  $R_{\text{day}}$  limits were used to classify the  $R_{\text{maxday}}$  maps, and the thresholds  $1,000 < R_{\text{day}} <$   
 226  $1,500 \text{ MJ.ha}^{-1}.\text{mm.h}^{-1}.\text{day}^{-1}$  and  $R_{\text{day}} > 1,500 \text{ MJ.ha}^{-1}.\text{mm.h}^{-1}.\text{day}^{-1}$  were also specifically used to analyze the

227 frequency of events causing natural disasters throughout the 21st century as they imply possible fatalities.  
 228 Therefore, the frequency of these events over the baseline and the three periods (1976-2005, 2011-2040, 2041-  
 229 2070, 2070-2099) was analyzed. It is possible to observe a slight change in the intervals considered to analyze  
 230 the frequency of these events used to map the  $R_{\text{maxday}}$  to consider periods of 30 years of data. Thus, 3900 events  
 231 were analyzed for each time slice, 30 for each of the 130 grid points generated by the 5-km Eta-HadGEM2-ES  
 232 model (Figure 1).

233 Figure 2 presents a flowchart with the steps to calculate the daily rainfall erosivity for the baseline and  
 234 time slices throughout the century and the conversion of these values to assess the rainfall hazards in MRRJ.



235  
 236 **Figure 2.** Flowchart with the methodology used to assess the rainfall hazards in MRRJ.

## 237 Results and Discussion

### 238 239 *Performance of the high-resolution climate model (5-km Eta-HadGEM2-ES model) to calculate rainfall* 240 *erosivity in the MRRJ*

241  
 242 To evaluate the high-resolution climate model in estimating daily rainfall erosivity, we examined its  
 243 capability to account for RUSLE's R-factor estimation, i.e., the long-term average annual rainfall erosivity, given  
 244 that R-factor values and patterns are well-known in the study region. Therefore, the R-factor for the ANA rain  
 245 gauges of Petrópolis, Nova Friburgo, and Teresópolis (Figure 1) was detailed. The R-factor calculated for these  
 246 three rain gauges using daily rainfall projected by the high-resolution climate model showed a good agreement  
 247 with the R-factor calculated based on the daily rainfall observed in the ANA rain-gauge stations. The R-factor  
 248 was 8,537; 10,554 and 7,639  $\text{MJ}\cdot\text{ha}^{-1}\cdot\text{mm}\cdot\text{h}^{-1}\cdot\text{year}^{-1}$ , respectively, to Petrópolis, Nova Friburgo, and Teresópolis,  
 249 using the observed daily rainfall. Considering the daily rainfall from the 5-km Eta-HadGEM2-ES climate model,  
 250 R-factor was 9,566 (an overestimate of 10.29%) to Petrópolis, 9,886 (an underestimate of 6.67%) to Nova  
 251 Friburgo, and 6,057  $\text{MJ}\cdot\text{ha}^{-1}\cdot\text{mm}\cdot\text{h}^{-1}\cdot\text{year}^{-1}$  (an underestimate of 15.82%) to Teresópolis. These results  
 252 demonstrate a good correspondence between the R-factor estimated based on the climate model and



253 observations. Furthermore, we can state that this model was able to cope with the strong orographic influence on  
 254 the rainfall in the region since the ANA rain gauges are located in different locations and altitudes of the MRRJ  
 255 (see isohyets contour in Figure 1).

256 Yin et al. (2013) demonstrated through 11 GCM simulations that the HadGEM2-ES model had the best  
 257 performance under surface conditions and atmospheric circulation (Chou et al., 2019). Furthermore, in analyzing  
 258 19 global climate models, Gulizia and Camilloni (2015) concluded that HadGEM2-ES presented the highest  
 259 spatial correlation between simulated precipitation values and those observed for South America in the baseline.  
 260 These studies support the 5-km Eta-HadGEM2-ES model to appraise erosivity events throughout the 21<sup>st</sup>  
 261 century. It is also needed to highlight the relevance of using a physical model for downscaling the outputs from a  
 262 GCM in mountainous regions to better capture the orographic effects (Chou et al., 2014a), which is a  
 263 considerable aspect of the MRRJ climate pattern.

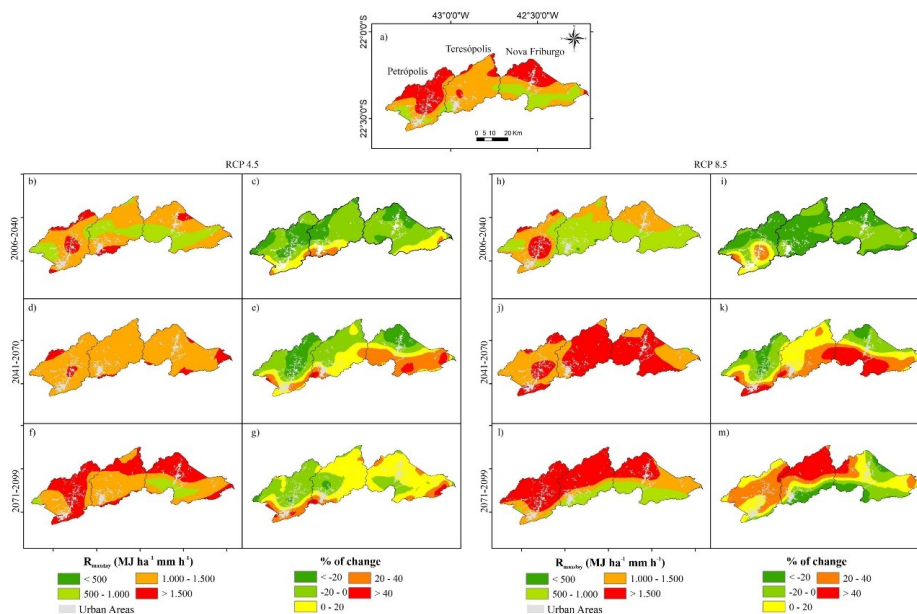
264 The estimation of  $R_{day}$  has been useful in identifying the most vulnerable areas to natural disasters and  
 265 analyzing the frequency of events associated with these disasters. Although the results of this study were only  
 266 applied to the MRRJ, the proposed methodological framework can be transferred to other vulnerable areas in the  
 267 country since there are data with a temporal resolution of 15 minutes for modeling  $R_{day}$ .

268

### 269 *$R_{maxday}$ mapping in the MRRJ throughout the 21<sup>st</sup> century*

270 Figure 3 shows the spatial distribution of  $R_{maxday}$  and its percentage variation throughout the 21<sup>st</sup> century  
 271 regarding the baseline in MRRJ considering the 5-km Eta-HadGEM2-ES model projections.  $R_{maxday}$  corresponds  
 272 to the maximum value calculated by considering a time series with at least 20 years of daily rainfall erosivity  
 273 (Mello et al., 2020).

274



275

276 **Figure 3.**  $R_{maxday}$  baseline map (a) and maps of the  $R_{maxday}$  and respective relative changes in relation to the  
 277 baseline throughout the 21<sup>st</sup> century (RCP4.5: b-g; RCP8.5: h-m).

278

279 Considering the baseline map (3a) and maps for the time slices in the RCP4.5 (3b - 3g), almost the  
 280 entire MRRJ is hit by rainfalls that result in  $R_{maxday}$  values that cause disasters with different consequences.

281 However, regardless of the climatic scenarios, the period with the most extensive spatial coverage of  $R_{\max\text{day}}$   
 282 values  $> 1,500 \text{ MJ}\cdot\text{ha}^{-1}\cdot\text{mm}\cdot\text{h}^{-1}\cdot\text{d}^{-1}$  is from 2070 to 2099 (Figures 3f – RCP4.5 and 3l – RCP8.5), especially for  
 283 the RCP8.5, where the positive relative changes (Figures 3l and 3m) dominate the north region of the largest  
 284 municipalities. Worthwhile that it is essential to highlight the concentration of these events in the urban areas of  
 285 Petrópolis and Nova Friburgo, which might result in fatalities.

286 The 2011-2040 time slice (Figures 3b and 3h, respectively, for RCP4.5 and RCP8.5) presented  $R_{\max\text{day}}$   
 287 values predominantly in the  $500 < R_{\max\text{day}} < 1,000 \text{ MJ}\cdot\text{ha}^{-1}\cdot\text{mm}\cdot\text{h}^{-1}\cdot\text{d}^{-1}$  class in Nova Friburgo and Teresópolis,  
 288 especially for RCP8.5 (Figure 3h). However, for this same time slice, an increase in  $R_{\max\text{day}}$  in Petrópolis in the  
 289 ranges that encompass values  $> 1,000 \text{ MJ}\cdot\text{ha}^{-1}\cdot\text{mm}\cdot\text{h}^{-1}\cdot\text{d}^{-1}$  were detected, meaning an increase in the magnitude of  
 290 the events that can potentially cause significant hazards and fatalities. Thus, in this time slice, which we are  
 291 crossing now, Petrópolis has been the most vulnerable municipality of the MRRJ to rainfall hazards. This aspect  
 292 has been observed recently (Alves et al., 2022).

293 Maps of the relative changes are also presented for both scenarios and were generated to understand the  
 294 spatial variation of  $R_{\max\text{day}}$  values regarding the baseline. Positive values mean an increase in  $R_{\max\text{day}}$ , and  
 295 negative values represent a decrease in magnitude. Compared to the baseline, there is a decrease in  $R_{\max\text{day}}$  for  
 296 the 2011-2041 time slice (Figures 3c and 3i). Except for the southern of the three municipalities and the  
 297 southwest and central region of Petrópolis, negative values were predominant, meaning a decrease in the  $R_{\max\text{day}}$   
 298 values in MRRJ throughout the century. Although this decrease,  $R_{\max\text{day}}$  still represents a very harmful situation  
 299 for MRRJ and needs to be considered carefully in the following decades.

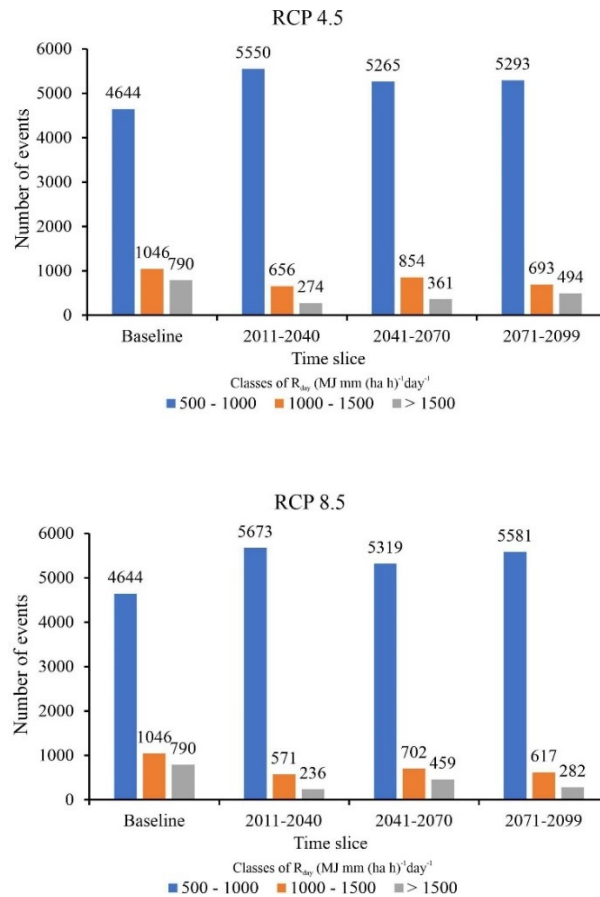
300 The 2011-2040 time slice projections are less uncertain than the other time slices as we are in the  
 301 middle of this period, allowing better initial conditions and assumptions for running the model (IPCC, 2022). In  
 302 this situation, we can expect an increase in the  $R_{\max\text{day}}$  values for areas of the MMRJ, requiring a careful  
 303 implementation of actions to minimize rainfall hazards, especially in the Petrópolis region.

304 These results imply that further attention to the areas that showed positive changes in  $R_{\max\text{day}}$  must be  
 305 implemented by the federal and state governments, focusing on the summer and spring periods as such areas are  
 306 the most vulnerable in the present to landslides and will be throughout the century. Actions like improving the  
 307 warning systems and meteorological and geological monitoring stations need to be expanded. In contrast, the  
 308 municipalities need to plan strategies to minimize fatalities, such as ready emergency staff that can respond  
 309 shortly to the crises and rethink the occupation of these areas in the middle term.

310

### 311 ***Frequency of the greatest $R_{\text{day}}$ events in MRRJ throughout the 21<sup>st</sup> century***

312 Figure 4 shows the frequency of  $R_{\text{day}}$  in the 130 grid points (Figure 1d) in MRRJ and another 86 in the  
 313 neighborhood, resulting in 216 points from the 5-km Eta-HadGEM2-ES outputs for the RCP4.5 and 8.5  
 314 scenarios. The range of the baseline and the climate projection data is 30 years for comparative purposes.



315  
 316 **Figure 4.** The frequency of the  $R_{\text{day}}$  projected by the 5-km Eta-HadGEM2-ES model that can result in natural  
 317 disasters in the MRRJ in the RCP4.5 (a) and 8.5 (b) scenarios for the baseline and the three different periods  
 318 throughout the 21<sup>st</sup> century.

319 The class with the highest frequencies, regardless of the RCP scenario and the period considered, is  
 320 between 500 and 1000  $\text{MJ}\cdot\text{ha}^{-1}\cdot\text{mm}\cdot\text{h}^{-1}\cdot\text{d}^{-1}$  (Figure 4). The events in this class represent 85, 81, and 82% of the  
 321 occurrences for the 2011-2040, 2041-2070, and 2070-2099 periods, respectively, for RCP4.5. Considering the  
 322 RCP8.5 scenario, 87, 82, and 86% of the events fall in this range, respectively. In the baseline, 72% of the events  
 323 were observed in this class. Greater frequencies in the RCP8.5 in relation to the RCP4.5, and for both scenarios,  
 324 were projected, i.e., significant increases regarding the baseline for this class. Therefore, climate change is  
 325 expected to increase the number of events in this class, highlighting that they can cause several damages,  
 326 fatalities included (Alves et al., 2022). Frequencies for this class for RCP8.5 were slightly higher than those for  
 327 RCP4.5, meaning a reduction of the events that can potentially cause hazards, following the classification  
 328 proposed by Alves et al. (2022) for MRRJ, i.e., a medium possibility to generate homelessly, damages on the  
 329 basic infrastructure and fatalities.

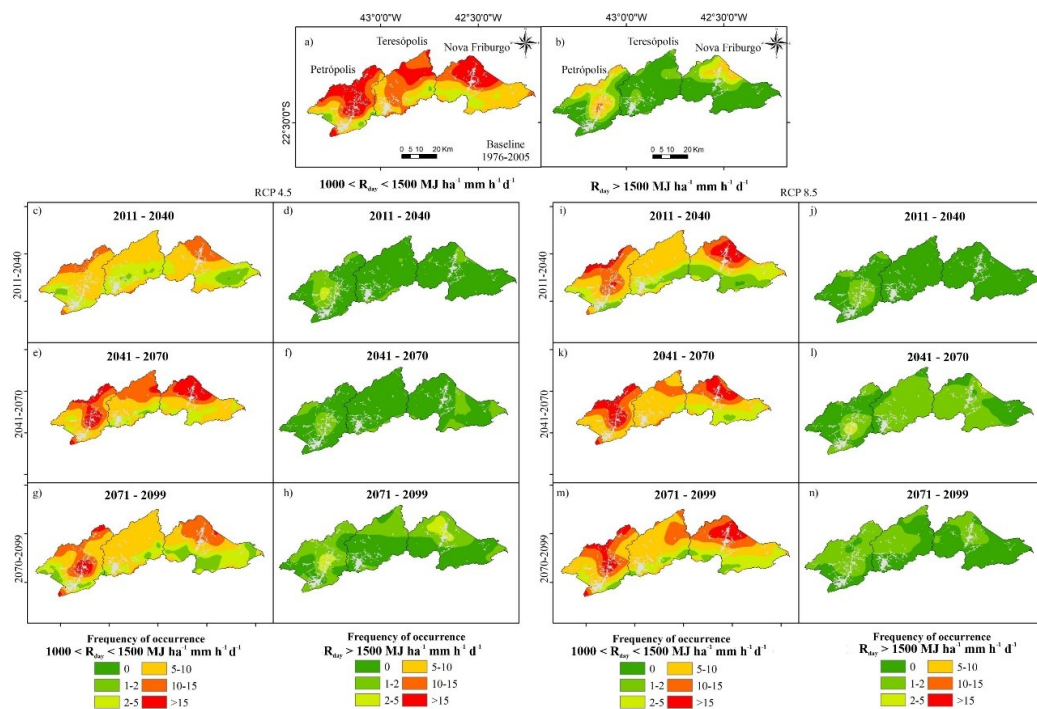
330 Oppositely, for the  $1,000 < R_{\text{day}} < 1,500 \text{ MJ}\cdot\text{ha}^{-1}\cdot\text{mm}\cdot\text{h}^{-1}\cdot\text{d}^{-1}$  class and RCP4.5 scenario, a higher  
 331 frequency throughout the 21<sup>st</sup> century than the RCP8.5 was projected. These events are related to the occurrence  
 332 of disasters with a "high" possibility of fatalities, a "very high" number of homeless people, and a "high"  
 333 possibility of causing damage to infrastructure and the economy. However, the behavior considering the three  
 334 analyzed periods was similar for the two scenarios, where the highest frequency of events in this class was  
 335 verified for the period from 2041 to 2070, being equal to 13% and 11% for the RCP4.5 and 8.5 scenarios,  
 336 respectively, and 16% for the historical period.

337 The  $R_{\text{day}} > 1,500 \text{ MJ}\cdot\text{ha}^{-1}\cdot\text{mm}\cdot\text{h}^{-1}\cdot\text{d}^{-1}$  class encompasses the harmost events, which have the lowest  
 338 frequency. In baseline, it was observed that 12% of these events, and throughout the 21st century, 4, 6, and 8%  
 339 for the RCP4.5 scenario in the 2011-2040, 2041-2070, and 2070-2099 time slices, respectively. Contrary to the  
 340 tendency observed for RCP4.5, in which there was a progressive increase throughout the 21st century (Figure  
 341 4a), the highest frequency observed for the RCP8.5 was in the 2041-2070 time slice, with 459  $R_{\text{day}}$  events  $>$   
 342  $1,500 \text{ MJ}\cdot\text{ha}^{-1}\cdot\text{mm}\cdot\text{h}^{-1}\cdot\text{d}^{-1}$ , representing approximately 7% of the total analyzed events.

343 Concomitantly analyzing the  $R_{\text{day}}$  classes related to natural disasters with "medium", "high" and "very  
 344 high" possibilities of fatalities and damage to infrastructure ( $R_{\text{day}} > 500 \text{ MJ}\cdot\text{ha}^{-1}\cdot\text{mm}\cdot\text{h}^{-1}\cdot\text{d}^{-1}$ ), it is observed that  
 345 the 2041-2070 time slice was the one with the highest frequencies for both RCP scenarios.

346 Mello et al. (2021) and Alvarenga et al. (2018) used the Eta-HadGEM2-ES in a resolution of 20 km to  
 347 simulate climate change impacts on streamflow in watersheds of the Southern Minas Gerais and Mantiqueira  
 348 Range region, which is in neighborhood MRRJ. In both studies, a decrease greater than 40% in the monthly  
 349 precipitation of the wet period, i.e., from January to April, was projected. In this study, we obtained a reduction  
 350 in the frequencies of the harmost  $R_{\text{day}}$  values ( $> 1,000 \text{ MJ}\cdot\text{ha}^{-1}\cdot\text{mm}\cdot\text{h}^{-1}\cdot\text{d}^{-1}$ ) of approximately 30% across the time  
 351 slices and RCP scenarios as a response to the reduction in the amount of monthly rainfall projected. However,  
 352 we can infer that there will be an increase in the concentration of rainfall in the wet period since a reduction in  
 353 the total monthly values is more significant than the frequency of extreme events. Thus, summer will continue as  
 354 the most dangerous rainfall disaster despite the reduced precipitation.

355 The spatial occurrence of critical  $R_{\text{day}}$  events throughout the 21<sup>st</sup> century considering the most severe  
 356 ones, i.e.,  $1000 < R_{\text{day}} < 1500 \text{ MJ}\cdot\text{ha}^{-1}\cdot\text{mm}\cdot\text{h}^{-1}\cdot\text{d}^{-1}$  and  $R_{\text{day}} > 1500 \text{ MJ}\cdot\text{ha}^{-1}\cdot\text{mm}\cdot\text{h}^{-1}\cdot\text{d}^{-1}$  classes are respectively  
 357 shown in Figure 5.



358  
 359 **Figure 5.** Frequency maps of events in the classes  $1,000 < R_{\text{day}} < 1,500 \text{ MJ}\cdot\text{ha}^{-1}\cdot\text{mm}\cdot\text{h}^{-1}\cdot\text{d}^{-1}$  and  $R_{\text{day}} > 1,500$   
 360  $\text{MJ}\cdot\text{ha}^{-1}\cdot\text{mm}\cdot\text{h}^{-1}\cdot\text{d}^{-1}$  projected by the 5-km Eta-HadGEM2-ES model in MRRJ for the baseline and RCP  
 361 scenarios.

362

363 The northern region of Nova Friburgo and the central region of Petrópolis are those with the highest  
 364 occurrences of  $R_{\text{day}}$ , for both RCP scenarios, in the  $1,000 < R_{\text{day}} < 1,500 \text{ MJ}\cdot\text{ha}^{-1}\cdot\text{mm}\cdot\text{h}^{-1}\cdot\text{d}^{-1}$  class (Figures 5a –  
 365 5g), being greater than 15 occurrences regardless of the time slice. However, between 10 and 15 events were  
 366 projected for both regions considering RCP4.5 in the 2011-2040 time slice.

367 Both scenarios have greater spatial coverage of the highest  $R_{\text{day}}$  values in the 2041-2070 time slice.  
 368 Compared to the baseline, it is predicted that there will be a decrease in such events in MRRJ in the 21st century.  
 369 This decrease is more noticeable for Teresópolis, where there was a greater frequency of events in the  $1,000 <$   
 370  $R_{\text{day}} < 1,500 \text{ MJ}\cdot\text{ha}^{-1}\cdot\text{mm}\cdot\text{h}^{-1}\cdot\text{d}^{-1}$  class for the baseline, whereas the frequency in this class from projections varies  
 371 from five to ten events.

372 The lowest frequencies were observed in the southern Nova Friburgo and Teresópolis and in the  
 373 southwest Petrópolis, where values were predominant between 1 and 5 events in the  $1,000 < R_{\text{day}} < 1,500 \text{ MJ}\cdot\text{ha}^{-1}\cdot\text{mm}\cdot\text{h}^{-1}\cdot\text{d}^{-1}$   
 374 class. This frequency class has a more considerable predominance from 2011 to 2040. The baseline  
 375 showed higher frequencies and spatial range of values within this  $R_{\text{day}}$  class. It is important to note that this  $R_{\text{day}}$   
 376 class is related to rainfall with a "high" possibility of fatalities, a "very high" number of homeless, and a "high"  
 377 possibility of damage to infrastructure and the economy. Thus, in the case of Petrópolis and Nova Friburgo,  
 378 although a decrease in the frequency of these events throughout the 21<sup>st</sup> century, it is understood that the highest  
 379 occurrences will prevail in urban areas for any period or RCP scenario. Therefore, it is necessary to establish  
 380 alert indexes and efficient public policies to mitigate the impacts caused by such events in the future. Although  
 381 Teresópolis presented a lower frequency of these events (5 to 10 events) throughout the century, this number of  
 382 events is high, meaning that this municipality can be hit by a rainfall event in this class once every three years in  
 383 the 2070-2099 time slice.

384 The frequency maps of events in the  $R_{\text{day}} > 1,500 \text{ MJ}\cdot\text{ha}^{-1}\cdot\text{mm}\cdot\text{h}^{-1}\cdot\text{d}^{-1}$  class showed a decrease regarding  
 385 the baseline. For RCP4.5, it is observed that there would be an increase in the occurrences in the 2070-2099 time  
 386 slice if compared to the baseline, where the projections for the urban areas of Petrópolis and Nova Friburgo vary  
 387 from two to five events. Considering the RCP8.5, this frequency of events was observed for the central region of  
 388 Petrópolis in the 2041-2070 time slice.

389 Based on the data analyzed and maps, Nova Friburgo and Petrópolis are the most vulnerable to natural  
 390 disasters with fatalities. However, a significant frequency of events in the  $1,000 < R_{\text{day}} < 1,500 \text{ MJ}\cdot\text{ha}^{-1}\cdot\text{mm}\cdot\text{h}^{-1}\cdot\text{d}^{-1}$   
 391 class may occur in Teresópolis, and events in this class can cause disasters with fatalities. Also, there is an  
 392 increase in the frequency of  $R_{\text{day}}$  values in the RCP8.5 compared to RCP4.5, except for the 2070-2099 time slice  
 393 considering the second  $R_{\text{day}}$  class analyzed (Figure 5m).

394 The  $R_{\text{day}}$  values calculated for the "mega-disaster" were equal to 900.1, 1962.8, and 2594.6  $\text{MJ}\cdot\text{ha}^{-1}\cdot\text{mm}\cdot\text{h}^{-1}\cdot\text{d}^{-1}$   
 395 for Petrópolis, Teresópolis, and Nova Friburgo, respectively, meaning greater impact on the last  
 396 municipality. Considering the  $R_{\text{day}}$  value  $>1962.8 \text{ MJ}\cdot\text{ha}^{-1}\cdot\text{mm}\cdot\text{h}^{-1}\cdot\text{d}^{-1}$  as the threshold for the "mega-disaster",  
 397 their frequency throughout the century was 87, 128, and 145 for RCP4.5, 74, 163, and 94 for RCP8.5, for the  
 398 2011-2040, 2041-2070 and 2070-2099 time slice, respectively, considering all grid points (Figure 1d). Thus,  
 399 with these events spatially distributed over MRRJ, the northern region of Nova Friburgo and the central region  
 400 of Petrópolis (both in their urban areas) will be the ones with the highest frequencies of events like the "mega-  
 401 disasters". Considering the grid points closest to Nova Friburgo and Petrópolis, five and nine "mega-disasters"  
 402 throughout the century for RCP4.5, and four and eight for RCP8.5, respectively, were projected. These "mega-

403 disasters" in both municipalities were projected for different years. Thus, a projection of 14 or 12 "mega-  
 404 disasters" occurring throughout the 21<sup>st</sup> century for the RCP4.5 and 8.5, respectively, could be projected, which  
 405 would increase to 17 and 15 when considering Teresópolis.

406 Our study sheds new insights into the influence of climate change on rainfall disasters. However, we  
 407 need to point out the limitations of our study that require future studies. For example, only one climate model,  
 408 downscaled by a physical model (ETA/CPTEC), was adopted here. Because the study region is a mountainous  
 409 area close to the Atlantic Ocean, i.e., the orographic effect is strong. Although the datasets used in this study are  
 410 unique for all of South America (5 km), the outputs downscaled in a more satisfactory resolution are  
 411 indispensable. Nevertheless, the uncertainties associated with the climate model exist, which should be  
 412 countered using additional models with 5-km resolution and the orographic aspect adequately solved by a  
 413 physical model.

414

#### 415 **Conclusions and future studies**

416 The studied region is one of Brazil's most vulnerable to extreme rainfall disasters. To overcome the  
 417 orographic effect on the rainfall in the region, we used the 5-km ETA/HadGEM2-ES model to analyze the  
 418 frequency of events that cause disasters, fatalities included. The datasets used in this study are from only one  
 419 global circulation model (GCM) dynamically downscaled to 5 km resolution. This aspect allowed capturing  
 420 orographic effects on rainfall spatial and temporal distribution. The Eta-HadGEM2-ES model is the unique  
 421 model available with such a resolution. Therefore, we can advance in terms of the uncertainty of the GCMs for  
 422 estimating extreme daily rainfall in an acceptable resolution for this purpose. Other GCMs have been considered  
 423 in South America but using a resolution of 20 km. Several studies have demonstrated no concordance among  
 424 them regarding extreme precipitation patterns over the century.

425 Another relevant study consists in evaluating how large-scale atmosphere drivers like multivariate  
 426 ENSO index, Southern Oscillation Index (SOI), Tropical Southern Atlantic Index (TSA), Pacific Decadal  
 427 Oscillation (PDO), Antarctic Oscillation (AAO), Atlantic Multidecadal Oscillation (AMO), and ENSO  
 428 precipitation index can impact extreme rainfall events that cause hazards in southeastern Brazil. For that, it is  
 429 imperative to expand a broader study regarding  $R_{\text{day}}$  modeling to assess statistical analyses, especially  
 430 multivariate ones (artificial intelligence, principal components analysis, Bayesian regression analyses, among  
 431 others), and establish possible connections.

432 In terms of conclusions, we can highlight:

- 433 e) The MRRJ presents high  $R_{\text{maxday}}$  values throughout the 21<sup>st</sup> century, showing a large coverage of  
 434 the extreme rainfall in MRRJ, especially from the first time slice.
- 435 f) The frequency of events in the moderate impact class ( $500 - 1,000 \text{ MJ mm (ha h)}^{-1}$ ) tends to  
 436 increase throughout the century, meaning fatalities will continue to occur in MRRJ, although in a  
 437 lower possibility.
- 438 g) The projection along this century is that 17 (RCP4.5) or 15 (RCP8.5) events of the same  
 439 magnitude, respectively, as the one that caused the "mega-disaster" in 2011 in MRRJ.

440

441

442

443 **References**

444

445 Alcântara, E., Marengo, J. A., Mantovani, J., Londe, L., San, R. L. Y., Park, E., Lin, Y. N., Mendes, T., Cunha,  
 446 A. P., Pampuch, L., Seluchi, M., Simões, S., Cuartas, L. A., Massi, K., Alvalá, R., Moraes, O., Filho, C. S.,  
 447 Mendes, R., and Nobre, C.: Deadly disasters in Southeastern South America: Flash floods and landslides of  
 448 February 2022 in Petrópolis, Rio de Janeiro, *Nat. Hazards Earth Syst. Sci. Discuss.* doi: 10.5194/nhess-2022-  
 449 163.

450

451 Alexander D, Gaillard JC, Kelman I, Marincioni F, Penning-Rowsell E, van Niekerk D, Vinnelli LJ  
 452 (2021) Academic publishing in disaster risk reduction: past, present, and future. *Disasters*, 45 (1), 5-18. Doi:  
 453 10.1111/disa.12432.

454

455 Alvalá RCS, Days MCA, Saito SM, Stenner C, Franco C, Amadeu P, Ribeiro J, Santana RASM, Nobre CA  
 456 (2019) Mapping characteristics of at-risk population to disasters in the context of Brazilian early warning  
 457 system. *Int. J. Disaster Risk Reduct.* 41, 101326. <https://doi.org/10.1016/j.ijdrr.2019.101326>.

458

459 Alves GJ, Mello CR, Guo L, Thebaldi MS (2022) Natural disaster in the mountainous region of Rio de Janeiro  
 460 state, Brazil: Assessment of the daily rainfall erosivity as an early warning index. *International Soil and*  
 461 *Water Conservation Research*, doi: [10.1016/j.iswcr.2022.02.002](https://doi.org/10.1016/j.iswcr.2022.02.002)

462

463 Amorim PB, Chaffe PB (2019) Towards a comprehensive characterization of evidence in synthesis assessments:  
 464 the climate change impacts on the Brazilian water resources. *Clim. Change* 1, 37-57.  
 465 <https://doi.org/10.1007/s10584-019-02430-9>.

466

467 André RGB, Marques VS, Pinheiro FMA, Ferraudo AC (2008) Identificação de regiões pluviometricamente  
 468 homogêneas no estado do Rio de Janeiro, utilizando-se valores mensais. *Rev. Bras. Meteorol.* 4, 501-509.  
 469 <http://dx.doi.org/10.1590/S0102-77862008000400009>.

470

471 Andrea KV, Nunes LH (2011) Impactos socioambientais associados à precipitação em municípios do litoral  
 472 paulista. *Geografia* 3, 571-588.

473

474 Bitar OY (2014) *Cartas de Suscetibilidade a Movimentos Gravitacionais de Massa e Inundações-1: 25.000: Nota*  
 475 *Técnica Explicativa*. IPT; CPRM, São Paulo.

476

477 Brasil. Ministério de Minas e Energia (2012) *Seleção dos Municípios Críticos a Deslizamentos: Nota*  
 478 *Explicativa*. CPRM, Rio de Janeiro.

479

480 Brito TT, Oliveira Jr JF, Lyra GB, Gois G, Zeri M (2016) Multivariate analysis applied to monthly rainfall over  
 481 Rio de Janeiro state, Brazil. *Meteorol. Atmos. Phys.* 5, 1-10. <https://doi.org/10.1007/s00703-016-0481-x>.

482

483 Calvello M, D'Orci RN, Piciullo L, Paes N, Magalhães M, Lacerda WA (2015) The Rio de Janeiro early  
 484 warning system for rainfall-induced landslides: Analysis of performance for the years 2010–2013. *Int. J.*  
 485 *Disaster Risk Reduct.* 12, 3-15. <https://doi.org/10.1016/j.ijdrr.2014.10.005>.

486

487 Cardozo CP, Monteiro AMV (2019) Assessing social vulnerability to natural hazards in Nova Friburgo, Rio de  
 488 Janeiro mountain region, Brazil. *REDER* 2, 71-83.

489

490 CEPED (2013) *Atlas Brasileiro de Desastres Naturais: 1991-2010, second ed.* Ceped, Santa Catarina.

491

492 Chen Y, Xu M, Wang Z, Chen W, Lai C (2020) Reexamination of the Xie model and spatiotemporal variability  
 493 in rainfall erosivity in mainland China from 1960 to 2018. *Catena*, 195, 104837.  
 494 <https://doi.org/10.1016/j.catena.2020.104837>.

495

496 Chou SC, Marengo JA, Lyra AA et al (2012) Downscaling of South America present climate driven by 4-  
 497 member HadCM3 runs. *Clim Dyn* 38, 635–653. <https://doi.org/10.1007/s00382-011-1002-8>.

498

499 Chou SC, Lyra A, Mourão C, Dereczynski C, Pilotto I, Gomes J, Bustamante J, Tavares P, Silva A, Rodrigues  
 500 D, Campos D, Chagas D, Sueiro G, Siqueira G, Marengo J (2014a) Assessment of climate change over South  
 501 America under RCP 4.5 and 8.5 downscaling scenarios. *American Journal of Climate Change*, 3, 512–527.  
 502 <https://doi.org/10.4236/ajcc.2014.35043>.

- 503  
504 Chou SC, Lyra A, Mourão C, Dereczynski C, Pilotto I, Gomes J, Bustamante J, Tavares P, Silva A, Rodrigues  
505 D, Campos D, Chagas D, Sueiro G, Siqueira G, Nobre P, Marengo J (2014b) Evaluation of the Eta  
506 simulations nested in three global climate models. *American Journal of Climate Change*, 3, 438–454.  
507 <https://doi.org/10.4236/ajcc.2014.35039>.
- 508  
509 Chou SC, Marengo JA, Silva AJ, Lyra AA, Tavares P, Gouveia Souza CR, Alves LM (2019) Projections of  
510 Climate Change in the Coastal Area of Santos. In: Nunes L., Greco R., Marengo J. (eds) *Climate Change in  
511 Santos Brazil: Projections, Impacts and Adaptation Options*. Springer, Cham. [https://doi.org/10.1007/978-3-  
512 319-96535-2\\_4](https://doi.org/10.1007/978-3-319-96535-2_4).
- 513  
514 Coelho Netto AL, Sato AM, Avelar AS, Vianna LGG, Araújo IS, Ferreira DLA, Lima PH, Silva APA, Silva RP  
515 (2013) January 2011: The extreme landslide disaster in Brazil. In: Margottini C, Canuti P, Sassa K. (Eds.),  
516 *Landslide Science and Practice*. Heidelberg, Springer, pp. 377-384.
- 517  
518 Dourado F, Arraes TC, Silva MF (2012) O Megadesastre da Região Serrana do Rio de Janeiro: As causas do  
519 evento, os mecanismos dos movimentos de massa e a distribuição espacial dos investimentos de reconstrução  
520 no pós-desastre. *Anu. Inst. Geociênc.* 2, 43-54. [http://dx.doi.org/10.11137/2012\\_2\\_43\\_54](http://dx.doi.org/10.11137/2012_2_43_54).
- 521  
522 Fernandes LG, Rodrigues RR (2018) Changes in the patterns of extreme rainfall events in southern Brazil. *Int. J.*  
523 *Climatol.* 3, 1337-1352. <https://doi.org/10.1002/joc.5248>.
- 524  
525 Flato G, Marotzke J, Abiodun B, Braconnot P, Chou SC, Collins W, Cox P, Driouech F, Emori S, Eyring V,  
526 Forest C, Gleckler P, Guilyardi E, Jakob C, Kattsov V, Reason C, Rummukainen M (2013) Evaluation of  
527 climate models. In Stocker TF, Qin D, Plattner GK, Tignor M, Allen SK, Boschung J, Nauels A, Xia Y, Bex  
528 V, Midgley PM (Eds.), *Climate change 2013: The physical science basis. Contribution of working group I to  
529 the fifth assessment report of the intergovernmental panel on climate change* (pp. 741–866). Cambridge, UK:  
530 Cambridge University Press. <https://doi.org/10.1017/CBO9781107415324.020>.
- 531  
532 Freitas CM, Carvalho ML, Ximenes EF, Arraes EF, Orlando J (2012) Vulnerabilidade socioambiental, redução  
533 de riscos de desastres e construção da resiliência: Lições do terremoto no Haiti e das chuvas fortes na Região  
534 Serrana, Brasil. *Ciênc. Saúde Coletiva* 17, 1577-1586. <https://doi.org/10.1590/S1413-81232012000600021>.
- 535  
536 Garcia MLT, Francisco CN (2013) Métricas da paisagem no estudo da vulnerabilidade da Mata Atlântica na  
537 região serrana fluminense–Nova Friburgo, RJ, in: XVI Simpósio Brasileiro de Sensoriamento Remoto. Inpe,  
538 pp. 3268-3274.
- 539  
540 Gulizia C, Camilloni I (2015) Comparative analysis of the ability of a set of CMIP3 and CMIP5 global climate  
541 models to represent precipitation in South America. *Int. J. Climatol.*, 35: 583-595.  
542 <https://doi.org/10.1002/joc.4005>.
- 543  
544 Holbig CA, Mazzone A, Borella F, Pavan W, Fernandes JMC, Chagas DJ, Chou SC (2018) PROJETA  
545 platform: accessing high resolution climate change projections over Central and South America using the Eta  
546 model. *Agrometeoros*, 26(1). <http://dx.doi.org/10.31062/agrom.v26i1.26366>.
- 547  
548 IBGE (2010) Census. [http://www.ibge.gov.br/home/estatistica/populacao/censo2010/  
549 default.shtm](http://www.ibge.gov.br/home/estatistica/populacao/censo2010/default.shtm) (accessed on  
550 January 17, 2020).
- 551  
552 Imbach, P., Chou, S.C., Lyra, A., Rodrigues, D., Rodriguez, D., Latinovic, D., Siqueira, G., Silva, A., Garofolo,  
553 L., Georgiou, S. (2018). Future climate change scenarios in Central America at high spatial resolution. *PLoS  
554 ONE*, 13(4), 1–21, doi: 10.1371/journal.pone.0193570.
- 555  
556 IPCC (2022) *Climate Change 2022: Impacts, Adaptation and Vulnerability. Contribution of Working Group II to  
557 the Sixth Assessment Report of the Intergovernmental Panel on Climate Change* Cambridge University Press.  
558 Cambridge University Press, Cambridge, UK and New York, NY, USA, 3056 pp.,  
559 doi:10.1017/9781009325844.
- 560  
561 IPCC (2013) *Climate Change 2013: The Physical Science Basis. Contribution of Working Group I to the Fifth  
562 Assessment Report of the Intergovernmental Panel on Climate Change*. Cambridge University Press,  
Cambridge and New York, 1535. <https://doi.org/10.1017/CBO9781107415324>.



- 563 Lukić, T., Gavrilov, M. B., Marković, S. B., Komac, B., Zorn, M., Mladjan, D., Đorđević, J., Milanović, M.,  
 564 Vasiljević, Dj. A., Vujičić, M. D., Kuzmanović, B., Prentović, R. (2013). Classification of the natural  
 565 disasters between the legislation and application: experience of the Republic of Serbia. *Acta Geographica*  
 566 *Slovenica* 53-1, 149-164.
- 567 Lukić, T., Micić-Ponjiger, T., Basarin, B., Sakulski, D., Gavrilov, M., Marković, S. B., Zorn, M., Komac, B.,  
 568 Milanović, M., Pavić, D., Minučer, M., Marković, N., Durlević, U., Morar, C., Petrović, A. (2021).  
 569 Application of Angot precipitation index in the assessment of rainfall erosivity: Vojvodina Region case study  
 570 (North Serbia). *Acta Geographica Slovenica*, 61(2), 123-153.
- 571 Lukić, T., Bjelajac, D., Fitzsimmons, K.E., Marković, S.B., Basarin, B., Mlađan, D., Micić, T., Schaetzel, J. R.,  
 572 Gavrilov, M.B., Milanović, M., Sipos, G., Mezősi, G., Knežević Lukić, N., Milinčić, M., Létal, A.,  
 573 Samardžić, I. (2018). Factors triggering landslide occurrence on the Zemun loess plateau, Belgrade area,  
 574 Serbia. *Environmental Earth Sciences*, 77, 519. <https://doi.org/10.1007/s12665-018-7712-z>.
- 575 Lyra A, Tavares P, Chou SC, Sueiro G, Dereczynski CP, Sondermann M, Silva A, Marengo J, Giarolla A (2017)  
 576 Climate change projections over three metropolitan regions in Southeast Brazil using the non-hydrostatic Eta  
 577 regional climate model at 5-km resolution *Theor Appl Climatol*. <https://doi.org/10.1007/s00704-017-2067-z>.
- 578 Machado RL, Carvalho DF, Rouws JRC, Gomes DP, Eduardo EN (2013) Erosividade das chuvas associada a  
 579 períodos de retorno e probabilidade de ocorrência no estado do Rio de Janeiro. *Rev. Bras. Ciênc. Solo* 2, 529-  
 580 547. <https://doi.org/10.1590/S0100-06832013000200024>.
- 581
- 582 Marengo JA, Chou SC et al. (2012) Development of regional future climate change scenarios in South America  
 583 using the Eta CPTEC/HadCM3 climate change projections: climatology and regional analyses for the  
 584 Amazon, São Francisco and the Paraná River basins. *Clim Dyn* 38, 1829–1848.  
 585 <https://doi.org/10.1007/s00382-011-1155-5>.
- 586
- 587 Mello CR, Ávila LF, Viola MR, Curi N, Norton LD (2015) Assessing the climate change impacts on the rainfall  
 588 erosivity throughout the twenty-first century in the Grande River Basin (GRB) headwaters, southeastern  
 589 Brazil. *Environ. Earth Sci.* 73, 8683-8698. <https://doi.org/10.1007/s12665-015-4033-3>.
- 590
- 591 Mello CR, Alves GJ, Beskow S, Norton LD (2020) Daily rainfall erosivity as an indicator for natural disasters:  
 592 assessment in mountainous regions of southeastern Brazil. *Nat. Hazards* 103, 947-966.  
 593 <https://doi.org/10.1007/s11069-020-04020-w>.
- 594
- 595 Mesinger F, Chou SC et al. (2012) An upgraded version of the Eta model. *Meteorol Atmos Phys* 116, 63–79.  
 596 <https://doi.org/10.1007/s00703-012-0182-z>.
- 597
- 598 Morar, C., Lukić, T., Basarin, B., Valjarević, A., Vujičić, M., Niemets, L., Telebienieva, I., Boros, L., Nagy, G.  
 599 (2021). Shaping Sustainable Urban Environments by Addressing the Hydro-Meteorological Factors in  
 600 Landslide Occurrence: Ciuperca Hill (Oradea, Romania). *International Journal of Environmental Research*  
 601 *and Public Health*, 18(9), 5022. <https://doi.org/10.3390/ijerph18095022>.
- 602
- 603 Oliveira NS, Rotunno Filho OC, Maton E, Silva C (2016) Correlation between rainfall and landslides in Nova  
 604 Friburgo, Rio de Janeiro—Brazil: A case study. *Environ. Earth Sci.* 20, 1-12. <https://doi.org/10.1007/s12665-016-6171-7>.
- 605
- 606 Pesquero JF, Chou SC et al. (2010) Climate downscaling over South America for 1961–1970 using the Eta  
 607 Model. *Theor Appl Climatol* 99, 75–93. <https://doi.org/10.1007/s00704-009-0123-z>.
- 608
- 609 Pinto LC, Mello CR, Norton LD, Pogger GC, Owens PR, Curi N (2018) A hydrogeological approach to a  
 610 mountainous Clayey Humic Dystrudept in the Mantiqueira range, southeastern Brazil. *Sci Agric.* 75, 60-69.  
 611 <http://dx.doi.org/10.1590/1678-992x-2016-0144>.
- 612
- 613 Ponjiger, T.M., Lukić, T., Basarin, B., Jokić, M., Wilby, R.L., Pavić, D., Mesaroš, M., Valjarević, A., Milanović,  
 614 M.M., Morar, C. (2021) Detailed Analysis of Spatial-Temporal Variability of Rainfall Erosivity and

- 615 Erosivity Density in the Central and Southern Pannonian Basin. Sustainability,  
616 13(23),13355. <https://doi.org/10.3390/su132313355>.
- 617 Reboita MS, Gan MA, Rocha RP, Ambrizzi T (2010) Regimes de precipitação na América do Sul: Uma revisão  
618 bibliográfica. Rev. Bras. Meteorol. 2, 185-204. <http://dx.doi.org/10.1590/S0102-77862010000200004>.
- 619  
620 Riquetti NB, Mello CR, Beskow S, Viola MR (2020) Rainfall erosivity in South America: Current patterns and  
621 future perspectives. Science of the Total Environment, 724, 138315.  
622 <https://doi.org/10.1016/j.scitotenv.2020.138315>.
- 623  
624 Silva LT, Rodriguez DA, Silva Britto JM, Siqueira Junior JL, Corte-Real JAM, Camarinha PIM (2016) A  
625 vulnerabilidade a escorregamentos de terra da bacia do rio Bengalas - Nova Friburgo - Brasil sob as  
626 projeções de mudanças climáticas do Eta-HadGEM-ES RCP 4.5. Revista Brasileira de Cartografia, 68 (9).  
627 Disponível em: <http://www.seer.ufu.br/index.php/revistabrasileiracartografia/article/view/44442>.
- 628  
629 Silva R, Mendes R, Fisch G (2020) Future scenarios (2021-2050) of extreme precipitation events that trigger  
630 landslides – a case study of the Paraitinga River watershed, SP, Brazil. *Ambiente e Agua - An*  
631 *Interdisciplinary Journal of Applied Science*, 15(7), 1-18. doi: <http://dx.doi.org/10.4136/ambi-agua.2558>.
- 632 van Vuuren DP, Edmonds J, et al (2011) The representative concentration pathways: an overview. Climatic  
633 Change 109, 5 (2011). <https://doi.org/10.1007/s10584-011-0148-z>.
- 634  
635 Webster, PJ (2013) Improve weather forecasts for the developing world. Nature 493, 17-19.  
636 <https://doi.org/10.1038/493017a>.
- 637  
638 Wischmeier WH, Smith DD (1958). Rainfall energy and its relationship to soil loss. Transactions of the  
639 American Geophysical Union 39, 285-291. <https://doi.org/10.1029/TR039i002p00285>.
- 640  
641 Yin L, Fu R et al. (2013) How well can CMIP5 simulate precipitation and its controlling processes over tropical  
642 South America?. Clim Dyn 41, 3127–3143. <https://doi.org/10.1007/s00382-012-1582-y>.
- 643  
644 Yu B, Rosewell CJ (1996) Rainfall erosivity estimation using daily rainfall amounts for South Australia. Aust. J.  
645 Soil Res. 5, 721-733. <https://doi.org/10.1071/SR9960721>.
- 646  
647 Zhang, W.B., Xie, Y., Liu, B.Y. (2002) Rainfall erosivity estimation using daily rainfall amounts (In Chinese).  
648 Scientia Geographica Sinica 22, 721–733.